UNIVERSITÉ DU QUÉBEC EN ABITIBI-TÉMISCAMINGUE

LE LABORATOIRE DE RECHERCHE TELEBEC EN COMMUNICATIONS SOUTERRAINES (LRTCS)

CARACTÉRISATION DU CANAL DE PROPAGATION BAN DANS UN MILIEU MINIER

MÉMOIRE PRÉSENTÉ À L'UNIVERSITÉ DU QUÉBEC EN ABITIBI-TÉMISCAMINGUE COMME EXIGENCE PARTIELLE DE LA MAÎTRISE EN INGÉNIERIE

PAR

MR MOULAY ELHASSAN ELAZHARI

JANVIER, 2015

DEDICATION

This thesis is dedicated to

My Mother

My Wife

And

My lovely Daughter

ACKNOWLEDGEMENTS

First and the foremost, I praise Almighty Allah and thank Him for bestowing His blessings upon me and enabling me to complete this work.

I also would like to thank my supervisor Professor Mourad Nedil for his support, resources, and guidance that he provided me during this work. I was especially touched by the kindness and the high ethics of professor Nedil.

Professors Khalida Ghanem and Ismail Ben Mabrouk have provided valuable inputs and gave me much appreciated directions during my papers redactions; I thank them a lot for their help and look forward to collaborate with them in future projects.

I would like to thank my mother, my wife, and my brothers for their support during my educational endeavor.

My friends (Mejdi and Reda) have always been supporting and kind to me.

Last, but not the least, I am very grateful to the LRTCS laboratory, for providing me the opportunity to pursue my MS degree.

Table of Contents

List of Figures

List of Tables

Acronyms and Abbreviations

IF	intermediate frequency
CDF	Cumulative Distribution Function
PDF	Probability Density Function
CSI	Channel State Information
dB	Decibel (ratio in log scale)
dBm	Decibel relative to 1 milliwatt
FFT	Fast Fourier Transform
IFFT	Inverse Fast Fourier Transform
GHz	Gigahertz
RMS	Root Mean Square
IEEE	Institute of Electrical and Electronics Engineers
ISM	Industrial Scientific and Medical
LOS	Line-of-Sight
NLOS	Non-Line-Of-Sight
MIMO	Multiple-Input Multiple-Output
SISO	Single-Input Single-Output
PDP	Power Delay Profile
PL	Path Loss
RF	Radio Frequency
RX	Receiver
TX	Transmitter
SNR	Signal-to-Noise Ratio
VNA	Vector Network Analyzer
WBAN	Wireless Body Area Network
BAN	Body Area Network

RÉSUMÉ

Le Body Area Network (BAN) est une technologie de réseau sans fil qui consiste à interconnecter, autour ou sur le corps humain des transmetteurs et des récepteurs afin d'établir une communication sans fil, impliquant le corps humain. À titre d'exemple, ces composants électroniques utilisant des courants de très faible puissance pourraient communiquer avec un centre de commande distant, pour alerter un service d'urgence. Les applications se trouvent principalement dans les domaines de la santé, militaire, et divertissement.

Cette technologie (BAN) pourrait être appliquée davantage dans un environnement minier en raison de sa simplicité et sa capacité à fournir des informations utiles telles que la surveillance de l'environnement ou d'état de santé des employés. En effet, les mineurs sont exposés quotidiennement à un certain nombre de risques qui affecte leurs santés. Dans le cadre de ce projet, nous proposons un système BAN efficace qui sera à la fois rentable et simple à utiliser dans une mine souterraine.

Ce projet de recherche consiste à déterminer, à la fréquence 2,4 GHz du standard IEEE 802.11, les performances des systèmes de communication SISO (Single Input Single Output) et MIMO (Multiple Input Multiple Output) pour les canaux BAN, en termes de l'étalement des retards (RMS delay spread), l'affaiblissement de parcours, la bande de cohérence et la capacité du canal.

Afin d'atteindre ces objectifs, une campagne de mesure a été effectuée dans une galerie de la mine CANMET (niveau 40m) en ligne de vue directe (LOS) et en ligne de vue indirecte (NLOS) en utilisant les topologies SISO et MIMO.

ABSTRACT

The Body Area Network (BAN) is a wireless networking technology that consists in interconnecting, on or around the human body, transmitters and receivers to establish wireless communication. For example, electronic components, mounted on the human body, using very low power could communicate with a remote control center to alert an emergency service. The BAN applications are mainly found in the areas of health, military, and entertainment.

This technology (BAN) could be applied in a mining environment because of its simplicity and its ability to provide useful information such as environmental conditions and employees' health status data. In fact, the miners are exposed daily to a number of risks that affect their health. As part of this project, we propose an efficient BAN system ,dedicated to the security of the miners, that is both cost effective and easy to use in an underground mine.

This research project consists in determining, at the 2.4 GHz frequency of the IEEE 802.11 standard, the performance of the SISO and MIMO communication systems for BAN channels, in terms of the RMS delay spread, the path loss, the coherence bandwidth and the channel capacity.

In order to achieve these objectives, measurement campaigns were carried out in the CANMET mine gallery (40m level) in line of sight (LOS) and no line of sight (NLOS) using SISO and MIMO topologies.

CHAPITRE 1

GENERAL INTRODUCTION

1.1) Introduction to the Master Project

Wireless communications have undergone tremendous growth. They were first used mainly by military and shipping companies and later quickly expanded into commercial use such as commercial broadcasting services (shortwave, AM and FM radio, terrestrial TV), cellular telephony, global positioning service (GPS), wireless local area network (WLAN), and wireless personal area network (WPAN) technologies. Today, these wireless communications systems have become an integral part of daily life and continue to evolve in providing better quality and user experience. One of the recent emerging wireless technologies is body area network (BAN).

Over the past years, this technology increasingly attracted a great deal of interest from academia, industry, and standardization bodies, because of the advances in process technologies and low cost integration solutions which opened the door to various applications of the (BAN) technology. In very broad terms, WBAN refers to the wireless communication technology encompassing the propagation at the on-body, off-body, and in-body channels. In the on-body channel, both the transmitter and the receiver are on the human body surface, whereas in the in-body channel the transmitter is within the body. In the off-body channel, the transmitter is located on the body, whilst the receiver is in the vicinity of the body. This growing technology has found many applications in the biomedical therapy, health care, sport, multimedia and entertainment, to use the body as a communication media or transmit the human vital signs [1].

There are many physical and environmental phenomena which affect the BAN signal propagation. The movement of the body parts, polarization mismatch, and scattering due to the body, will cause fading of the signal. Shadowing of the links and reflections from the

body parts will also cause fading. Multiple signal paths on the body, such as the two possible paths from front to back around the body from both sides, will also cause fading.

Additionally, the surrounding environment will cause fading, such as fading due to the floor or ground, and fading due to local environment, such as furniture, walls of a room, machinery in a mine gallery...etc.

In addition to fading, another very important concern for on-body communication is the transmitted power, which is to be kept as low as possible. 0 dBm is still believed to be a high transmit power for the body area networks. Reducing power level allows increasing the battery life and reducing the Specific Absorption Rate (SAR) value, which is highly desirable [2].

Applications of the BAN technology is increasingly finding grounds in personal healthcare, entertainment, security and personal identification, fashion, and personalized communications, which drives research to establish more reliable and efficient link between the devices mounted on the body. The current standards for wireless communications like Bluetooth [2, 3], Zigbee [2, 4], and BodyLAN [2, 5] are already operating but there is still much room for improvement.

Moreover, multiple antennas for the on-body and off-body channels is an optimal solution for providing high data rate and reliable transmission between the body-worn wireless devices and sensors, such as in military applications, sports and entertainment, and patient monitoring systems.

In fact, for optimal communication, it is necessary to minimize fading and increase the output signal to noise ratio (SNR) without increasing the transmit power, which is an advantage of using MIMO systems. In these systems, antenna diversity, also known as space diversity, is a well-known solution toward overcoming fading and providing a power efficient link in mobile communications, and hence improving the quality and reliability of a wireless link. The channel capacity can be significantly increased through the use of multiple-input multiple-output (MIMO) techniques which are useful for high data rate applications. The use of MIMO techniques for on-body communications has received little attention, as much of the work on body-centric communication focuses on the antenna design [2,6], channel characterization [2, 7, 8], and the effect of human body presence on the link performance. Some preliminary measurements are reported with two monopole antennas at the receiver end

for on-body channels in [2, 9, and 10]. Additionally, first and second order statistics and some diversity results for channels with wearable receiving antennas where the transmitter is at a fixed position in the room are presented in [11, 12], thus characterizing the off-body channels and some on-body channels as well.

Moreover, many researches have been carried out to investigate the performance of the off-body channels at the 2.45 GHz ISM (industrial, scientific and medical) band, in the past few years, benefitting from the development of devices miniaturization technology [13]. Various other articles in the literature deal with on body communication systems, for patients' vital signs monitoring application [13].

In general, much of the works on WBAN multiple-input multiple-output (MIMO) systems concerns the characterization of MIMO on-body channels, while the MIMO off-body channel characterization was somewhat neglected [14, 15]. This may have been due to the fact that ensuring a communication in off-body channels may be challenging because of the short range nature of the used devices.

On the other hand, there has been a growing interest in implementing MIMO systems in indoor environments, because of their now proven efficiency in offering high data rate and low error rate communications [8, 16-18]. In fact, while MIMO systems have been extensively investigated for applications in tunnel roads and subways in the last few decades, the study of such systems in underground mines is still limited [16]. Benmabrouk et Al. have thoroughly investigated the use of MIMO systems in a mine gallery in the 2.45 GHz ISM band, for conventional radio transmission, using different kinds of antennas, namely the monopole and the patch antennas [19]. Interesting results were driven to show the capacity improvement relative to SISO case due to the exploitation of MIMO capabilities in both line of sight (LOS) and no line of sight (NLOS) applications. Even more, the effect of the mining machinery was taken into consideration in [19].

This Master report is concerned with the on-body and off-body communication inside a mine gallery where the transmitter is worn by the mine worker, whereas the receiver is either on the body or at a close proximity from the body.

Analyzing the performance of MIMO system in the mining environment which includes a lot of scattering objects, reflecting metals and shadowing structures, affecting both the path gain and the time dispersion of the link, is not an easy task because of the so-mentioned

particularities of the BAN channel. Adding to this, the effect of the human body as implied by the on-body and off-body communication studied herein in underground channels is even more challenging. To the best of the authors' knowledge, no study of the MIMO neither on-body nor off-body channel characterization in a mining environment was reported yet in the literature.

Therefore, in this thesis report, the characterization and capacity evaluation of the 2×2 MIMO and SISO off-body channels are investigated in underground environment at the 2.45 GHz band. The effect of directivity is sought by using monopole and patch antennas for both LOS and NLOS situations. First, the channel impulse responses are evaluated for different locations of the access points relative to the body. The path loss is then determined and plotted for different distances between the transmitter and the receiver and the path loss exponent is derived. Moreover, the channel capacity is calculated from the measurements similarly to [20] and [21]. The capacity study in both scenarios aims at showing the effect on the MIMO link capacity of a strong LOS component and multipath propagation. Moreover, the relationship between the average capacity and the average SNR is also highlighted. The coherence bandwidth and RMS delay spread are also derived and discussed.

In the on-body section of the report, the performance of SISO and MIMO WBAN systems, in a mine gallery, is comparatively evaluated at the 2.45 GHz ISM band. Three on-body channels (Belt-Head, Belt-Chest, and Belt-Wrist) were characterized with the body at different postures. The channel capacity was derived from the measurements similarly to [20] and [14], and then compared for the three on-body channels. The RMS delay spread, and the coherence bandwidth were also derived (similarly to [21]) and compared for different measurement scenarios.

1.2) Problem

Recently, there has been a great deal of focus in establishing communication on or around the body. In body-centric communications, communication is established through nodes which are placed on the body, or close to it, communicating with each other or with other nodes positioned apart from the body such as base stations or central data storage devices. Wired connection of the nodes is inconvenient because it can obstruct the free motion. The use of special fabrics, would allow the user to move comfortably, but it may not

be desirable to wear due to fashion preferences of the user. Other proposed methods include body current mechanism and near field communication. Body current method uses the emission of electric field on the surface of the body to use it as a transmission path [2]. Near-Field communication uses magnetic field induction for very short-range communication [2]. None of these two techniques is suitable for high data rate applications (like video streaming and multimedia). Wireless connectivity with antennas is therefore a very suitable choice.

Among the major issues that should be considered in body area communications are the antenna design and performance, channel characterization, the effect of human body presence and movement, and the transmitted power. A wearable antenna should be low profile, light weight and comfortable for the body surface [22]. The wearable RF components should also be able to support a high data rate transmission and should have low power consumption. Therefore, the use of a high enough frequency and a highly efficient link is required [2]. Moreover, for effective design and understanding of the channels, the knowledge of electromagnetic properties of the human body is essential.

In addition to the previously mentioned problems, wireless communication systems in an underground environment should be designed to provide reliable services with high throughput. However, the conventional communication systems, using a single antenna for transmission and reception SISO have a capacity limited by the transmission power and the bandwidth of the radio link [23]. Additionally, communication systems centered on the human body are limited in transmission power [24]. Therefore, radio systems that are centered on the human body can benefit from the application of MIMO architecture to improve capacity [14]. Moreover, it is well known that the performance of MIMO systems depends on the conditions of the radio channel, which differs from one medium to another; this justifies the need to study the on-body and off-body channels in a mine, highlighting the impact on the capacity due to the use of MIMO systems. For a complete characterization of these channels, several channel parameters should be determined (such as: RMS delay spread, coherence bandwidth, path loss exponent, and fading).

1.3) Objective of the research project

In this master's project, the multiple-input multiple-output (MIMO) off-body and on-body channel capacity is investigated in the underground mine untypical indoor environment

and compared to the SISO system using the same type of antenna element. Monopole and patch antennas were used in the measurements campaigns in order to study the effect of antenna directivity on the capacity of such channels. Furthermore for the off-body scenario, both line of sight (LOS) and no line of sight (NLOS) scenarios are of interest and the off-body channel is characterized in terms of the channel impulse response, path-loss, RMS delay spread, and coherence bandwidth. In On-body experiments, three On-body channels were characterized in terms of the channel impulse response, RMS delay spread, coherence bandwidth; the channel capacity was also determined. The variation of these parameters in the different measurement scenarios was also discussed.

1.4) Research methodology

To meet the BAN communication system requirements in an underground mining environment, we used the following methodology:

- In the first phase, we conducted a state of the art by focusing mainly on the characterization of the on-body and off-body channels in indoor environments and on the use of MIMO topology in mining media to improve the capacity of the propagation channel.

- In the second phase, a measurements campaign was conducted in the CANMET gold mine near Val d'Or in Canada as shown in figure 1-1 and figure 1-2. The environment mainly consists of very rough and dusty walls, floor, and ceiling. The temperature is about 6° C in a highly humid environment. There is mining machinery few meters away from the measurements' setup; the ceiling includes many metal rods and is covered with metal screens. In order to characterize the off-body SISO and MIMO channels propagation in this mine gallery at the 2.45 GHz band, the transmitting antennas were placed at a fixed position in the middle of the mine pathway (40m underground). The receiving antennas were placed on the right side of the chest of a 1.80m, 75Kg male subject wearing a miner's outfit. Two types of MIMO antennas were used during the measurements, namely a 2×2 MIMO monopole antenna set and a 2×2 MIMO patch antenna set; therefore the impact of antenna directivity was addressed. Both the transmitting and the receiving antenna elements are separated by a half wavelength distance, thus approximately 6 cm. During the measurements, 6

data snapshots were collected at each distance, from a distance of 1m through 5m away from the transmitter, as shown in figure 1-2. The transmitting and receiving antennas were connected to the two ports of the previously calibrated vector network analyzer (VNA). At each snapshot, the S_{21} values were recorded for 6401 frequency samples around the center frequency of 2.45 GHz. The noise floor for the measurements was considered at -90 dBm. In the on-body measurements, three on-body channels were considered for the measurements. For each on-body channel, the transmitting antenna set (TX) was placed at the left side position of the belt. The receiving antenna set (RX) was placed alternatively at the right side of the chest (RX 1), the right side of the head (RX 2), and at the right wrist position (RX 3), thus forming three on-body channels: belt-chest, belt-wrist, and belt- head as shown in figure 1-2. The transmitting antenna set was placed to point upward, and the receiving antenna set was pointing downward. The distance between the body and the antenna was kept at about 5-10 mm. The transmitting and receiving antennas were connected to the two ports of the vector network analyzer (VNA), after calibrating the VNA with the cables connected to it. Figure 1-2 shows the human test subject and antenna connections in the mine environment.

- Finally, after getting the S-parameters, using simulation software MATLAB, we have determined the parameters of the channel such as: the path loss, the coherence bandwidth, the RMS delay spread, and the capacity of the channel.

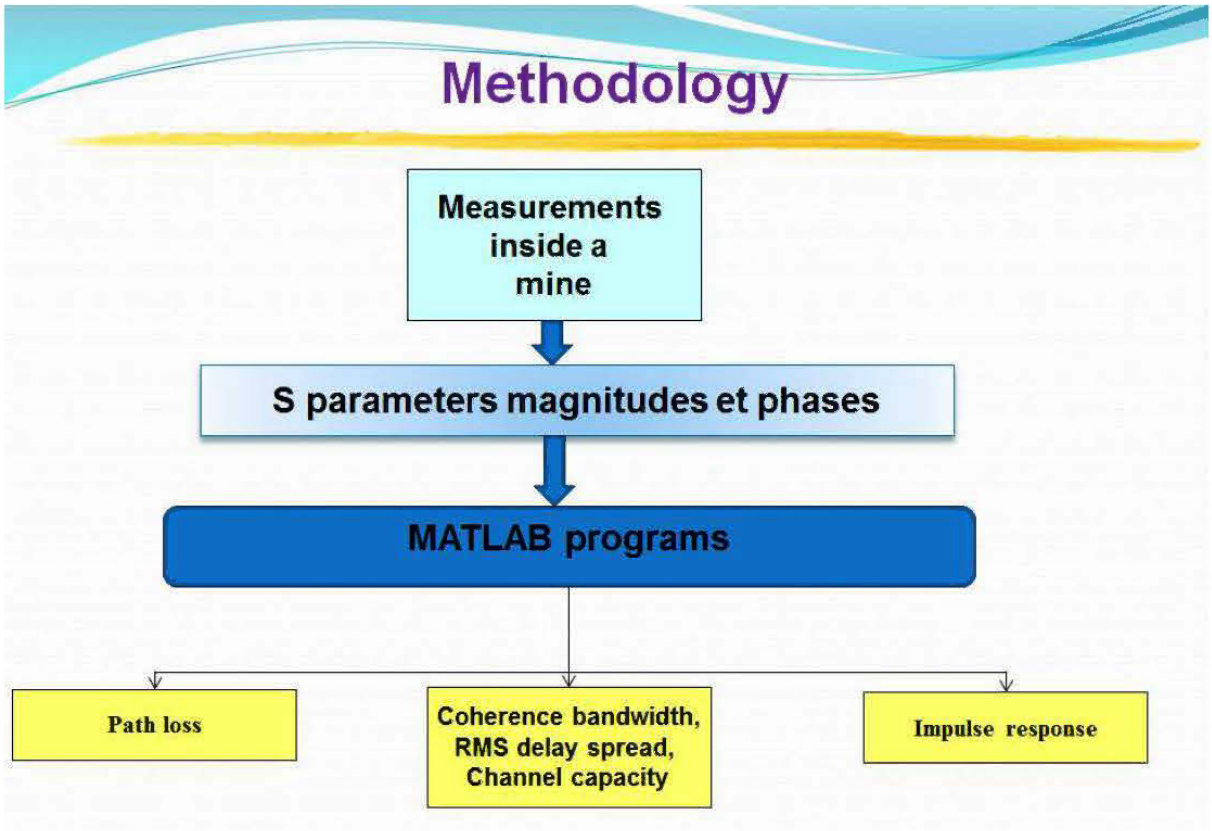

Figure 1- 1. Research methodology block diagram

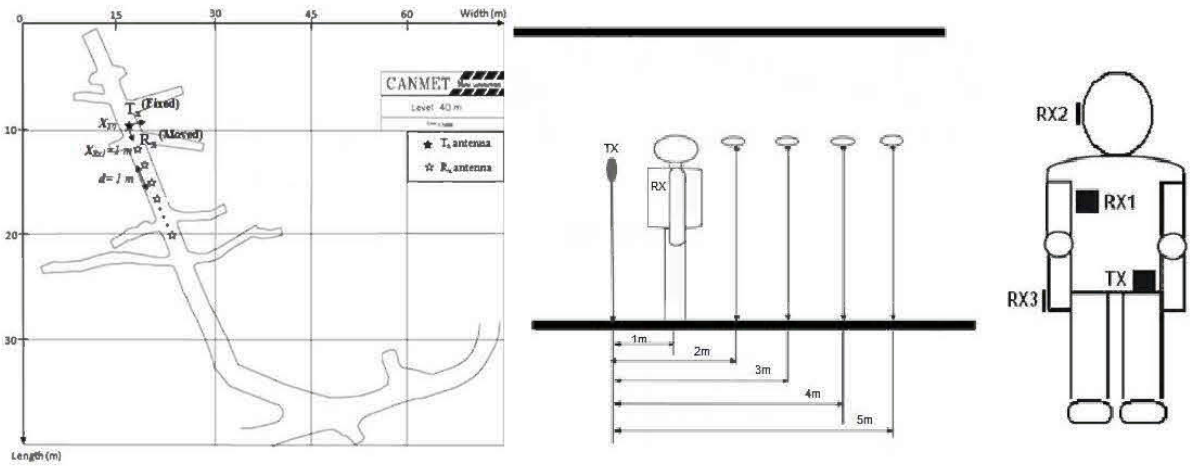

Figure 1- 2. Measurement setup

1.5) Thesis structure

In this thesis report, we present the following topics:

Chapter 2 provides an introduction to body area network. It briefly reports the applications of this technology and the different phenomena affecting the propagation at this channel. The different types of WBAN technology are summarized.

Chapter 3 provides an overview of the MIMO systems. It theoretically describes the MIMO channels through the channel matrix, and talks about the MIMO capacity.

Chapter 4 comparatively discusses the different types of diversity. It defines the diversity gain parameter as a mean to quantify the benefits of the different diversity techniques.

Chapter 5 gives an overview of the channel characterization types and the parameters that are usually used to characterize the propagation channels. It talks in detail about the fading as the main issue affecting the electromagnetic signal propagation. Finally, the chapter briefly introduces the different types of channel modelling.

Chapter 6 details the research methodology. This includes a description of the environment, measurement equipment and measurement methods. Mounting antennas on the body, to constitute various on-body channels, is discussed and the details of the measurement setup for the on-body and off-body experiments are given. The movements performed during the measurements are also described.

Chapter 7 discusses the different results obtained for the on-body and off-body sets of measurements inside the CANMET mine. It combines the results from the different measurement scenarios to determine and discuss the different channel parameters including the channel impulse response, path-loss, RMS delay spread, and coherence bandwidth.

Chapter 8 summarizes the derived conclusions and opens the door for Future Work possibilities.

1.6) Conclusion

This chapter consisted of an introduction to the master project, which aims to characterize the SISO and MIMO channels inside a mine gallery. It presented the problems associated with a WBAN communication system inside a mine and briefly mentions the techniques used to combat these problems. The objectives of the research project have been detailed, and the methodology followed to achieve them is described. In subsequent chapters, some back ground information related to the different themes of the master project is presented, starting by an overview of the WBAN technology in chapter 2.

CHAPTER 2

OVERVIEW OF THE BODY AREA NETWORK

2.1) Wireless body area network (WBAN) technology overview

Body-centric communication is established through nodes which are placed on the body, or close to it, communicating with each other or with other nodes (such as base stations or central data storage devices) positioned at a close proximity from the body.

2.1.1) On-body technology

The on-body technology is a kind of body area network (BAN) communication technology that found many applications in personal health care, entertainment, military, firefighting and many other fields [25].

In the on-body channels, both the transmitter and receiver move and change their position in the scattering environment and with respect to each other. Perhaps the most significant phenomenon affecting the on-body communication is channel fading, which occurs during normal activity, due to the dynamic nature of the human body, the multipath around the body, and the scattering by the environment. This fading can be mitigated through the use of diversity.

On-body communication applications are linked to several fields, such as medical-sensor networks, emergency-service workers, and entertainment. This technology also received a great deal of interest from the defense department, in order to wirelessly connect on-body soldier equipment. The medical field exhibits different uses for the on-body technology such as: Medical implants, patient monitoring and diagnostic systems, and personal health care. Some published reports demonstrated the strong interest of the defense field in the on-body technology, in terms of interconnecting various subsystems on a soldier [26]; It was found

that the Line of sight (LOS) was established reliably (most of the scattering is directed away from the body). Moreover, high path loss attenuation was observed in a link through the torso due to the human shadowing [26].

Other application areas for the on-body technology include: security, police, sports training, fire fighters, personal identification, fashion, and personalized communications as seen in figure 2-1.

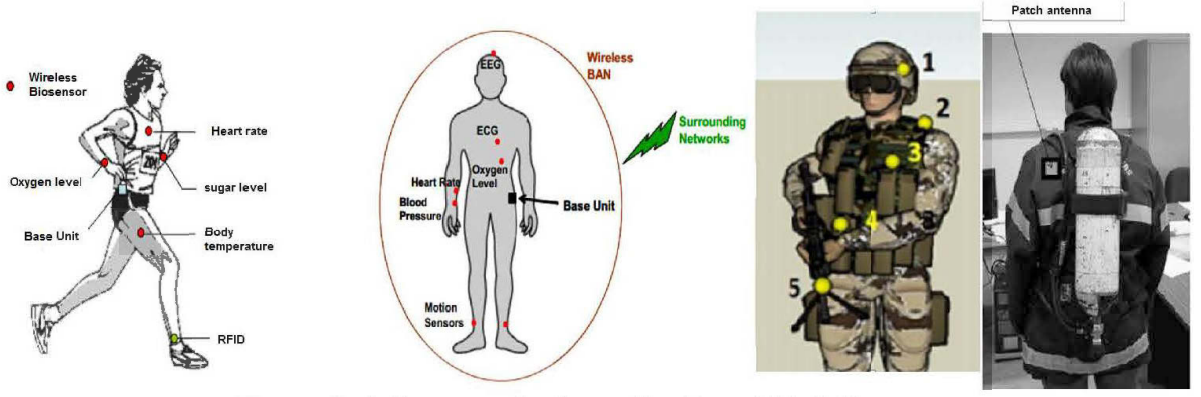

Figure 2- 1. Some on-body applications [24, 26].

2.1.2) Off-body technology

The off-body technology deals with the communication link between devices mounted on the body, and other devices, or access points, away from the body. It found application in the industrial and medical fields. Examples of this technology include wearable RFID tags, and body-worn sensors to and from the data acquisition system or server, for a medical support network with wireless sensors placed on the body; figure 2-2 represents some of the off-body applications. Careful attention should be taken in antenna design, placement, and orientation. The antennas should have radiation patterns directed away from the body, providing all-round coverage and must be isolated from the body to avoid the effect of human body on the antenna performance [2]. Indeed, the most important factor that affects the quality of propagation in the off-body technology is the shadowing effect, which causes fading. This is due to the pedestrian movement that obstructs the off-body radio link and results on multi-path disturbance. It was found that using multiple antenna techniques reduces the influence of pedestrian effects on off-body radio-links [27].

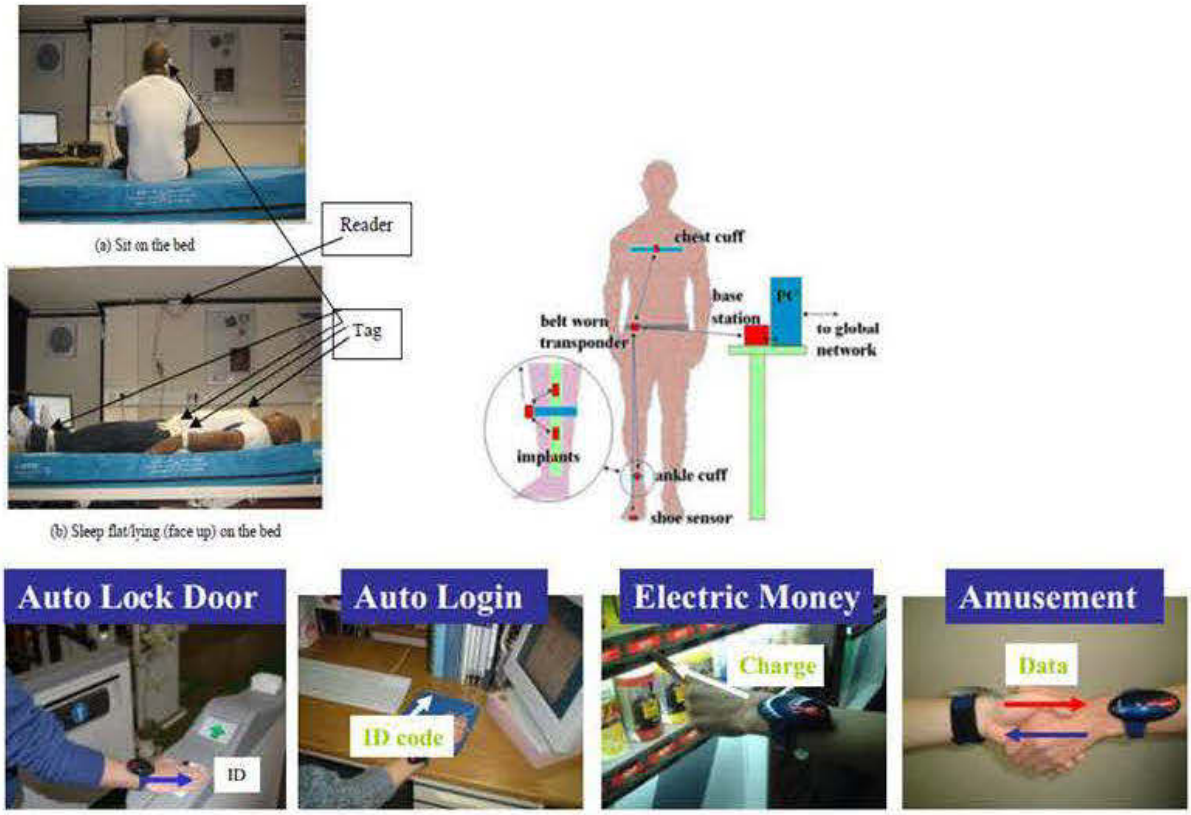

Figure 2- 2. Some off-body applications [2, 57].

2.1.3) On/Off-body technology

On/Off-body communication is another technology that is of interest to many fields including health care and military. This communication's link combines the characteristics and challenges of the on-body as well as the off-body link. For example, this link will require antennas that can support the two technologies (on-body and off-body communication). This is very challenging because the on-body link requires a polarization pattern that is parallel to the body surface, while the off-body link requires one that is directed away from the surface. The challenge is further aggravated when moving toward microwave frequencies where the path loss is greater and antenna design and orientation should be carefully taken care of [2]. A possible solution is to design a configurable antenna that can work either in the on-body mode or the off-body mode by using microwave switches embedded in the device. This idea was cleverly applied in [27] with a design of an aperture coupled microstrip patch antenna that is fed using stripline. The antenna changes its functionality from the on-body mode to the off-body mode using switches and is able to attain a return loss that remains below -30 dB

throughout the entire operating frequency with a linear increase of the path loss from -0.39 dB at 1 GHz to -1.65 dB at 4 GHz.

2.1.4) In-body technology

The in-body technology consists of one or more TX-RX link through the human body. Benefitting from the new microelectronic technological achievements, it found interesting applications in the medical field where implantable medical devices, communicating with the outside world, are put inside the human body. Examples of these devices include the heart pacemakers and retinal implants [2].

2.2) WBAN technology normalization

Efforts have been made to develop standards for the WBAN and an IEEE task group, IEEE 802.15.6 (IEEE 802.15.BAN), has been established for this purpose in November 2007. This task group is the sixth task group of the IEEE 802.15 working group.

IEEE 802.15 is a working group of the Institute of Electrical and Electronics Engineers (IEEE) 802 standards committee which specifies Wireless Personal Area Network (WPAN) standards [2]. It includes seven task groups and one interest group for Terahertz called IGTHz. In December 2011, the task group 802.15.6 or 802.15.BAN and task group 802.15.7 developed new standards for BAN and Visible Light Communication (VLC), respectively. IEEE 802.15.1, first published in June 2002, is a standard for WPAN based on Bluetooth, whereas, 802.15.2 provides recommendations for the coexistence of the WPANs and Wireless Local Area Networks (WLAN) [2]. More details about other task groups of IEEE 802.15 are given on its website.

2.3) Antennas for WBAN channels

The 2.45GHz channel allows the use of smaller antennas, because the wavelength for this channel is in the range of few centimeters (about 12 cm). This advantage in the dimension comes with complexity of the design for a WBAN channel. The requirements for antenna design at 2.45 GHz for WBAN applications could be summarized as follows.

A wearable antenna should be low profile, light weight and comfortable for the body surface [22]. The antenna should have a high enough gain to offset the path loss that characterizes the WBAN channels, but not too high to be harmful. In fact, some antenna characteristics (such as the radiation patterns and gain) may change drastically in the presence of a high loss medium such as the human body [2].

In order to maximize coupling between body-worn devices, the maximum of the radiation pattern should be tangential to the body's surface (creeping waves propagation) [22]. However, in this case, the wave polarized parallel to the body will attenuate faster than the perpendicular polarized one [2]. For off-body communication, the pattern must be directed away from the body. Omni-directional radiation pattern antennas (such as the monopole antenna) placed tangential to the surface of the body are generally considered suitable for on-body applications, when taking in consideration the gain reduction due to the presence of the body [2]. For on-body applications, where the wave propagates along the surface of the body as creeping wave and is attenuated much more rapidly compared to the free space [2], the antenna must be designed for a minimum SAR. This could be achieved by by the use of a suitable ground plane of the antennas to reduce back radiation [2]. Careful attention should be done during the design to insure a low reflection coefficient at the desired frequency even when the antenna is mounted on the body, taking in consideration that detuning could occur in the presence of the human body [2].

Comparative studies of various antennas (such as the rectangular patch, monopole, PIFA, and circularly polarized patch antenna) were performed and the antennas parameters were compared in [29, 30]. According to those studies, some antennas can perform well in some aspects, and perform badly in other aspects. The monopole antennas, beside their disadvantageous shape, exhibit the best path gains. The patch antennas have the advantage of their low profile shape and are more stable in terms of mismatch, but do not provide a satisfactory link performance. The textile wearable antennas are the best in terms of weigh and shape, they are flexible and could have comparable performance to conventional printed antennas [2].

2.4) Human body modeling and phantoms

Developing BAN systems in the GHz range may benefit from the development of experimental phantoms emulating the dielectric properties of human skin in order to accurately characterize the on-body propagation channel; this requires an accurate estimation of the absorption of the electromagnetic power by the human body.

It is important to know that the dielectric properties of the human body are frequency dependent. Moreover, the penetration depth of the lower frequencies is higher than that of the higher frequencies [2]. The penetration depth and conductivity for muscle and fat tissues are shown in figure 2-3.

As it's seen from figure 2-3, the penetration depth at 2.45 GHz is much smaller compared to low frequencies; hence, at this frequency, the propagation will likely be confined to the surface of the body, especially at small transmitted powers.

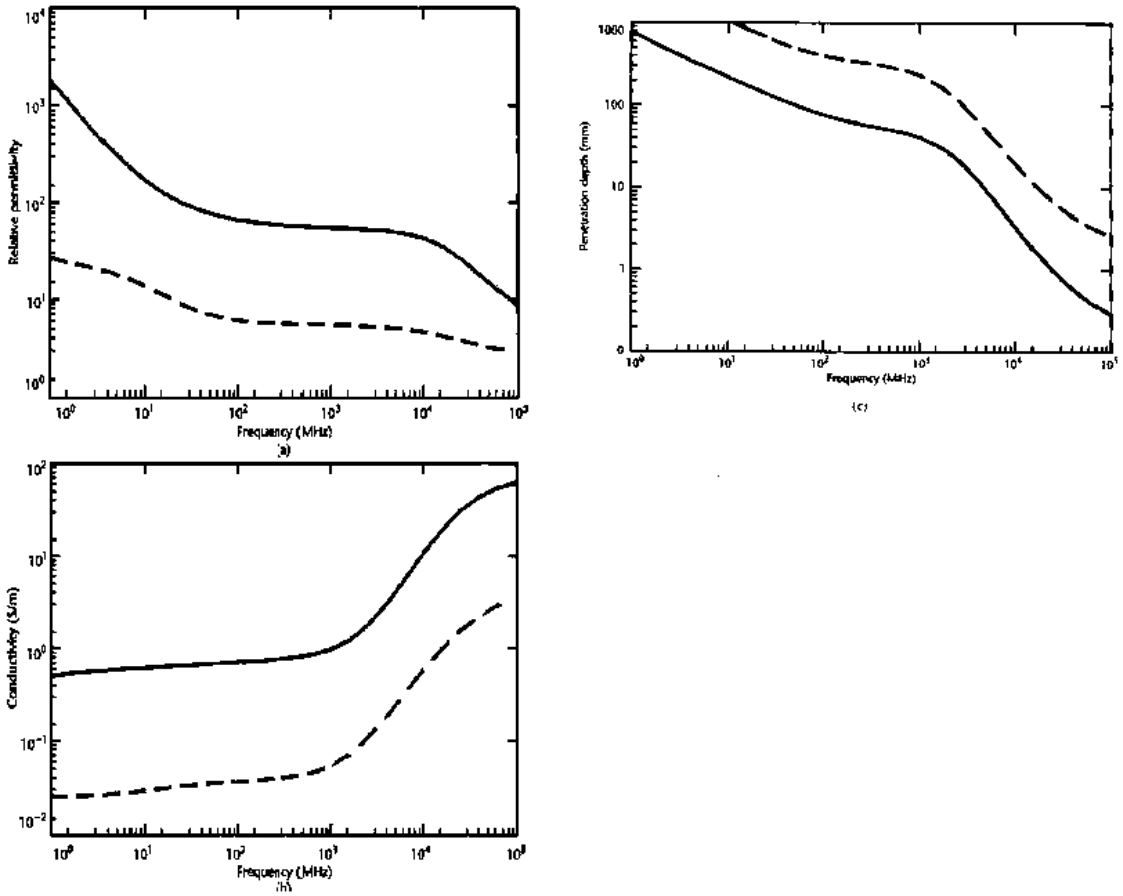

Figure 2- 3. Electromagnetic properties of Muscle (solid line) and Fat (dotted line) tissues with respect to frequency (a) Relative Permittivity (b) Conductivity and (c) Penetration depth [2].

Determining the dielectric properties of the human skin is the first step toward building a 2.45-GHz equivalent phantom. Three types of physical phantoms are presented in the literature, namely, the liquid, semisolid, and solid phantom [2]. The three types differ upon complexity, frequency usage, and durability.

Firstly, liquid phantoms are homogenous phantoms that represent a convenient way to simulate the body. They are well suited for measurements in the 30-MHz–6-GHz range but cannot be used at millimeter range because of the Shell [31]. Semisolid phantoms do not require any bounding container and have been used for antenna and on-body channel characterization [31]; They are especially useful to simulate organs with high water content like muscle and brain etc [2]. Finally, solid or dry phantoms have the advantage of keeping their shape for a long period of time and have stable characteristics. These phantoms can be built from a single organ phantom to whole body phantoms, depending upon the application.

2.5) Conclusion

In this chapter, WBAN technology has been explained. Four types of systems were discussed, namely the on-body, off-body, on/off-body, and in-body technologies. The particularity of the WBAN systems, which enforces different restrictions on the antenna design, was discussed. Finally, different types of phantoms emulating the dielectric properties of human skin were presented comparatively. Some other concepts mentioned in the introduction shall be the subject of further clarification throughout this manuscript, including the MIMO systems which are explained in the next chapter.

CHAPTER 3

OVERVIEW OF MIMO SYSTEMS

3.1) MIMO channel

The limitations of SISO systems (containing a single transmit antenna and a single antenna at the reception), due to the richness of multipath in a confined space such as a mine, have led researchers to consider alternative solutions in order to improve the capacity of the wireless systems. Hence, several studies have concluded that a system with multiple antennas at the transmission and at the reception takes advantage of the multipath to considerably improve the capacity of the radio link compared to a SISO system [32].

In fact, MIMO techniques are known to significantly improve the reliability of wireless systems by lowering the bit error rate (BER), improving the signal to noise ratio, and enhancing the capacity of the system. This could be achieved through diversity which proved to be powerful in lowering fading and improving the BER [2, 24, 33]. Diversity provides the best results when the fading at the different branches is uncorrelated and the branch signals have the same average power [33]. Usually, the higher order MIMO schemes are able to achieve the best performance in terms of BER. It was shown that a 4×4 MIMO using space time codes, provide a better BER performance than a 2×2 or a 1×1 MIMO [24].

MIMO technology allows increasing the capacity of the wireless system without an increase in bandwidth. This increase in capacity is limited by the correlation and power imbalance among the spatial sub-channels, mutual coupling between the spatially separated antennas, and the presence of a strong direct link between the transmitter (Tx) and receiver (Rx) in the line-of-sight (LOS) transmission [34]. In an interesting on-body research, using two different models of three MIMO on-body channels each (using PIFA antennas), ergodic capacity performance has been examined in [35]. Results show that the belt head channel is comparable to a Rayleigh distribution, while the belt-chest exhibits a loss in MIMO capacity because of the presence of a strong LOS component [35].

Figure 3-1 shows that MIMO systems offer a number of advantages in comparison to the SISO system having a single transmitting antenna and a single receiving antenna for an on-body application used by fire fighters [24].

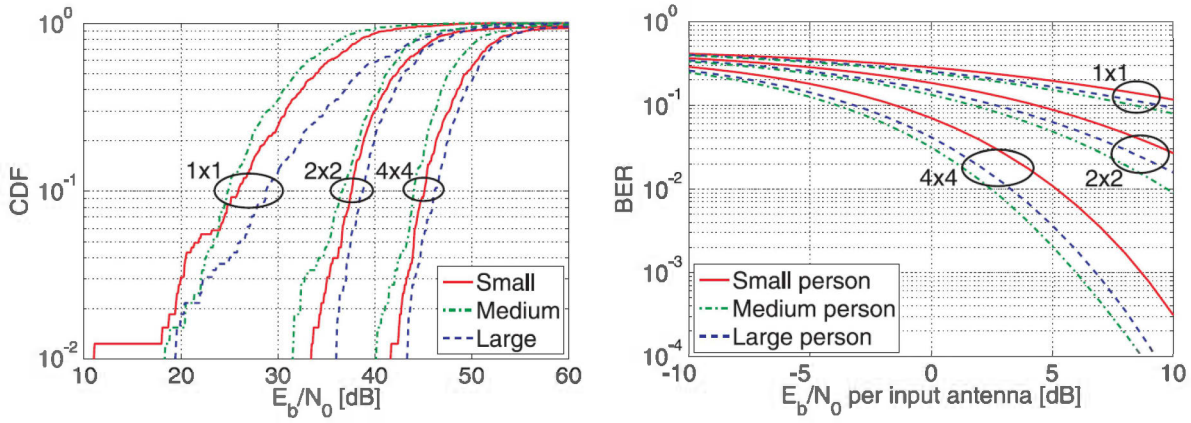

Figure 3- 1. Improvement in terms of BER and SNR for MIMO systems with respect to SISO systems for on-body application used by fire fighters using three different body sizes [24]

In general, it is demonstrated that MIMO systems (shown in figure 3-2) have the ability to turn multipath propagation, traditionally a disadvantage of wireless transmissions in a benefit to the user. They benefit from the random fading [36, 37], and the multipath [38, 39], for the purpose of expanding the transfer rates.

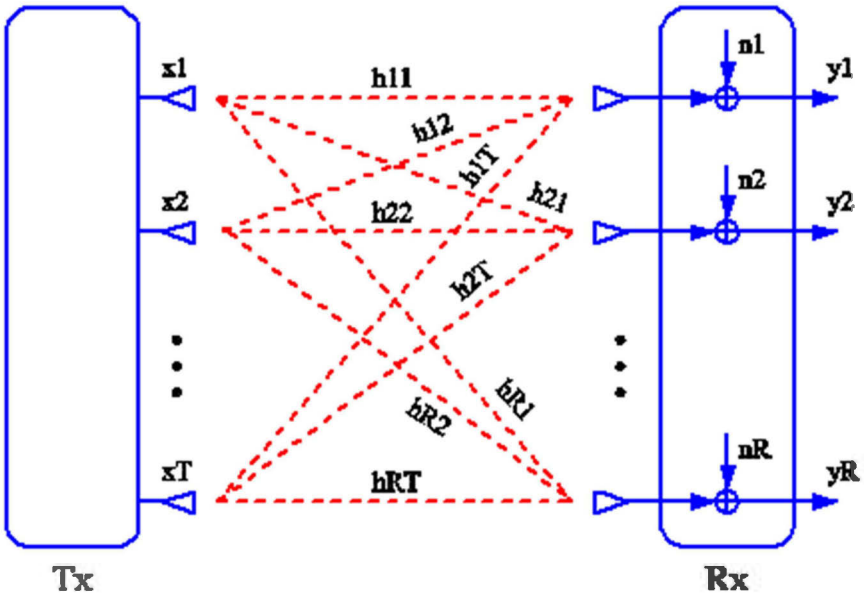

Figure 3- 2. Block diagram of a MIMO system [40]

3.2) MIMO matrix

The MIMO input-output relationship between m transmit and n receive antennas is described by the following equation [14]:

$$Y=HX+N \qquad (3\text{-}1)$$

where X is the [m × 1] transmitted vector, Y is the [n × 1] received vector, N is the receive additive white Gaussian noise (AWGN) vector, and H is the n × m channel matrix which for the case of the 2×2 MIMO considered channel is reduced to

$$H=\begin{bmatrix} h_{11} & h_{12} \\ h_{21} & h_{22} \end{bmatrix} \qquad (3\text{-}2)$$

where h_{ij} is the complex random variable that represents the complex sub-channel gain from the ith transmitting antenna to the jth receiving antenna. In our measurements, the values of the parameters S_{21} correspond to the different h_{ij} values.

3.3) Correlation of the branch signals

The correlation of the branch signals greatly affects the performance of a MIMO receiver. When the correlation is low, the branch signals fade differently, allowing an increase in the ergodic capacity at the receiver [2]. For most of the mobile communication scenarios, correlation coefficient of 0.7 is considered suitable [33]. One useful measure of the branch correlation is the complex signal correlation coefficient ρs, wich contains both the phase and amplitude correlation.

$$\rho_S = \frac{\sum_{i=1}^{N} V_1(i)\, V_2{}^*(i)}{\sqrt{\sum_{i=1}^{N} V_1(i)\, V_1{}^*(i)}\sqrt{\sum_{i=1}^{N} V_2(i)\, V_2{}^*(i)}} \qquad (3\text{-}3)$$

Where V_1 and V_2 represent the zero-meaned complex voltage signals of port 1 and 2, respectively and N is the total number of samples [2].

3.4) MIMO channel capacity

The channel capacity is a measure of the theoretical maximum data rate per unit of bandwidth that can be reliably transmitted through a certain channel [41].

In this thesis report, the MIMO channel capacity is used to measure the performance of the MIMO link taking in consideration the effect of the SNR and the multipath richness.

Channel ergodic capacity for a regular SISO configuration is calculated using the well-known Shannon formula [20]:

$$C_{SISO}[bps/Hz] = log_2(1 + \rho|H|^2). \qquad (3\text{-}4)$$

Where H is the normalized channel response and ρ is the average signal to noise ratio (SNR).

Similarly, the channel capacity with MIMO configuration is computed using the following formula [14]:

$$C_{MIMO}[bps/Hz] = log_2(\det[\boldsymbol{I}_n + \frac{SNR_{av}}{m}\boldsymbol{H}\boldsymbol{H}^*]) \qquad (3\text{-}5)$$

Where $\boldsymbol{H}$ is the normalized $m \times n$ channel response (m ≥ n), SNR_{av} is the average signal to noise ratio, $\boldsymbol{I}_n$ is the $n \times n$ identity matrix, and * represents the complex conjugate transpose. In our case, $\boldsymbol{H}$ matrix is normalized such that at each realization, the square of its Frobenius norm is equal to the product of its dimensions ($\|H\|_F^2 = nm$) [42, 43].

The Frobenius normalization method allows investigating the multipath richness of the environment [14]. The outage capacity, which is calculated from the CDF curves at a certain probability, ideally follows a Rayleigh distribution of the envelopes when subchannels of the MIMO system are independent and identically distributed (iid) and hence perfectly uncorrelated. This is however not true for practical systems, especially in the presence of a strong LOS component [14, 19].

3.5) Conclusion

In this chapter, the theoretical study of a MIMO communication system is presented. Then, the capacity formula for a SISO and a MIMO configuration was explained. Thus, MIMO systems seem very beneficial for wireless communications, since the maximum theoretical bit rate increases with the number of antennas used, without any increase of the transmitted power, or the bandwidth of the signal. Therefore, it is now clear that our solution which consists of implementing and studying a MIMO WBAN system in underground mines, is clearly justified. While, we only used space diversity in this project, we are presenting the different kinds of diversity schemes, in the next chapter, to get the reader to understand this concept and appreciate its implementation in our project.

CHAPTER 4

DIVERSITY OVERVIEW

Diversity refers to a method for improving the reliability of a communication system by using multiple communication channels to send or receive information [2]. Diversity is a well-known technique in combatting fading and co-channel interference and improving the bit error rate [2, 24, 33]. Diversity techniques benefit from the fact that different channels experience different levels of fading and interference to improve the gain and capacity of the system. The multipath richness is exploited to improve the diversity gain. The general idea is to use multiple uncorrelated branches with statistically independent fading characteristics. When the different channels are sufficiently separated in time, frequency, space, radiation pattern, and / or polarization, the fading on the individual channels will be independent due to the different channel conditions; hence, with proper combining of the branches, the SNR can be improved due to the deep fades reduction [2]. Figure 4-1 depicts an example of diversity at the reception.

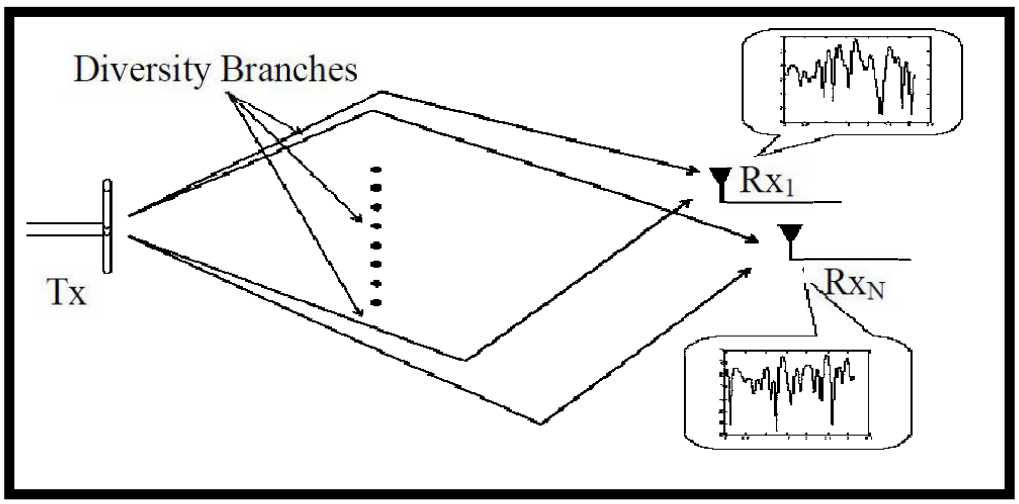

Figure 4- 1. Diversity at the reception [2].

4.1) Types of diversity

Diversity can be applied in several ways:

- Antenna diversity or space diversity, is a type of diversity that uses two or more antennas at the transmission or/and at the reception to improve the wireless link quality and reliability, by exploiting the multipath richness of the environment. It is mainly effective in urban and indoor environments where there is rarely a clear line-of-sight (LOS) [2]. The multipath components usually exhibits phase shifts, time delays, attenuations, and distortions and can destructively interfere with one another at a receiver. Space diversity, because of its inherent multi-view of the received signal, is effective at mitigating these multipath issues. In fact, the signal will fade differently at each antenna. Thus if one antenna experience a deep fade, it is unlikely that the other antennas will behave in the same manner. Hence the overall performance of the link is improved [2].
- Time Diversity consists of sending the same amplitude samples at different time slots. When the time slots separation is high enough (at least the reciprocal of the fading bandwidth), the sequential amplitude samples of the fading signal will be uncorrelated [2].
- Frequency Diversity consists of transmitting the signal over several frequency channels with a separation that is necessarily greater than the coherence bandwidth [2].
- Pattern Diversity consists of using directional antennas at either at the transmitter or at the receiver (such as a beam switching array). The radiation patterns are directed in different angles undergoing different fading, and hence uncorrelated; ideally the different patterns should have a minimum overlap and a combination of patterns similar to an Omni-directional pattern [2].
- Polarization diversity consists of transmitting and receiving multiple versions of a signal through antennas having different polarizations. A difference between the polarized components received at the receiver usually called the cross-polarization discrimination (XPD), must be low for effective polarization diversity to get a high diversity gain [2].

4.2) Comparing the different types of diversity

This section examines the differences between the different types of diversity as presented in [44]. This investigation showed that using spatial, polarization, or pattern diversity, diversity gains of 7–10 dB are achievable at the 99% probability level. Diversity gain of 8 to 9 dB is typical in NLOS indoor and outdoor channels using antenna spacings as small as 0.1–0.15λ [44]. The same research indicates that polarization diversity configurations can increase SNR by 12 dB or more in certain cases by eliminating polarization mismatch. In general, space diversity performs better than other types of diversities when the incoming angles of arrival are uniform such as in the open surface communications. Space or pattern diversity outperform the polarization diversity in a situation where the transmitted wave is not heavily depolarized (such as the LOS situations) due to a high XPD [2]. In NLOS scenario the performance of the polarization diversity is comparable to that of a space diversity [2]. Polarization diversity has the advantage over space diversity in terms of economizing the cost because it can be designed using a single multi-polarization antenna, contrary to the space diversity [2].

4.3) Diversity gain

One parameter which measures the improvements in the signal strength, SNR, or BER due to the use of diversity is diversity gain. It provides a good incite on the improvement in the communication quality due to diversity. Diversity gain is measured at a certain outage probability (usually 1% or 10% probability level), by comparing the values of the signal strength, for example, of the diversity combined signal with that of the strongest branch signal as seen in figure 4-2 [2].

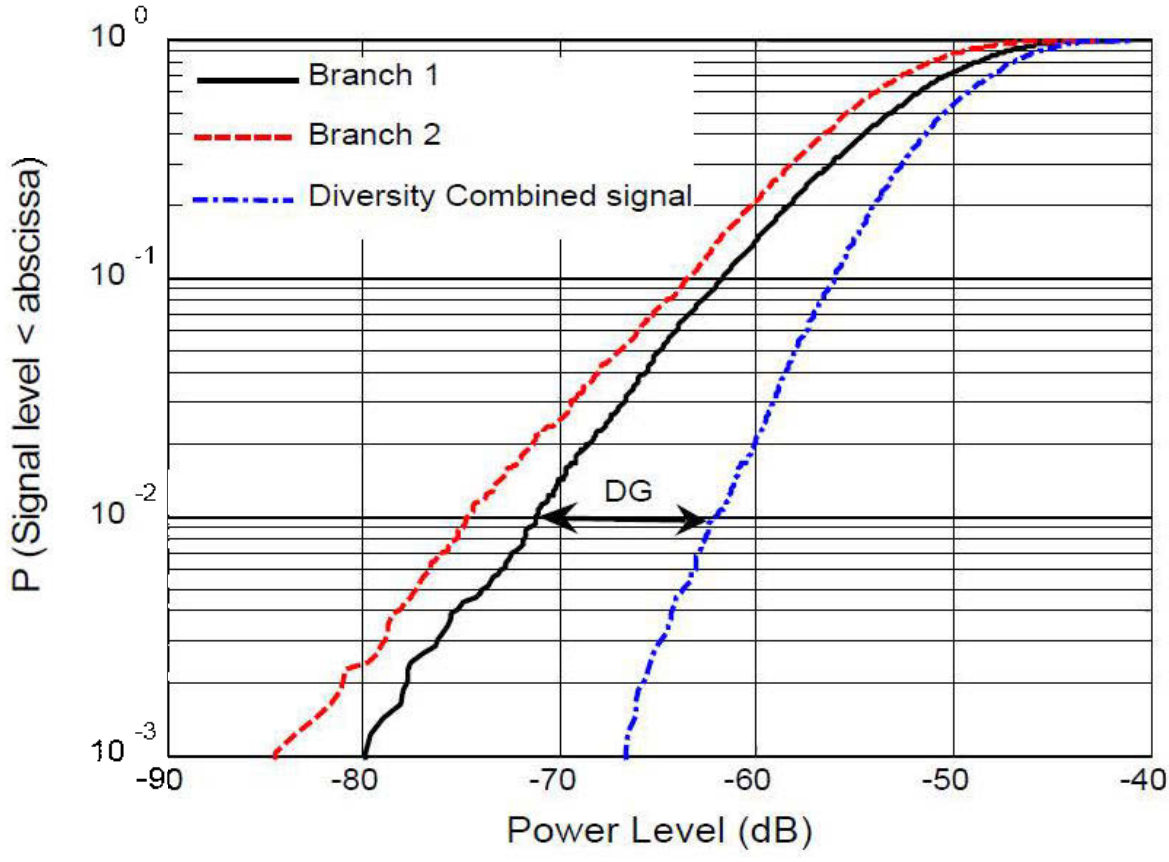

Figure 4- 2. Diversity gain calculation [2]

Diversity gain is defined as follows:

$$DG = \frac{P_{div}}{P_{ref}} \qquad (4\text{-}1)$$

$$DG = P_{dBdiv} - P_{dBref} \ (dB) \qquad (4\text{-}2)$$

where P_{div} , P_{ref} , P_{dBdiv} , and P_{dBref} are respectively the power level of the diversity combined signal, the power level of the reference signal (which is strongest among the branch signals) and those same parameters expressed in dBs at a certain probability level. Diversity gain can also be presented in terms of SNR or BER and is inversely dependent upon the correlation and the power difference among the branch signals [44, 45, 46]. Results from experimental investigations and comparison of antenna diversity techniques for on-body and off-body radio propagation channels show that for rich multipath environment the diversity gain is higher for the non-line of sight cases compared to the line-of-sight scenarios; it was also observed that off-body diversity is almost 50% more efficient than on-body diversity (50% more DG for the off-body) [47].

4.4) Conclusion

In this chapter, we presented an overview of diversity which is used to improve the performance and overcome fading. This requires a sufficient separation of the different channels in time, frequency, space, radiation pattern, and / or polarization, in order to achieve deep fades reduction and an overall improvement in SNR. Different types of diversity have been compared, and the diversity gain parameter has been introduced as a mean to measure the improvements in the signal strength. While the previous sections talked about the WBAN systems and the importance of diversity for a good WBAN communication, the next section will talk about the core concept of this project, which is the channel characterization.

CHAPTER 5

CHANNEL CHARACTERIZATION OVERVIEW

When an electromagnetic wave propagates through a radio channel, it is affected by diverse phenomenon, affecting its quality and sometimes severely harming the communication link. These propagation issues are generally attributed to reflection, diffraction, and scattering, which will be discussed in the following sections. In indoor environments as it is the case for a mine gallery, the direct line of sight path is sometimes obstructed by the different objects and natural obstacle potentially causing a severe diffraction loss. As a result, multiple reflections occur allowing a multitude of paths of different lengths, between the transmitter and the receiver. At the receiver, the beams arriving through the different paths will interact causing multipath fading at a specific location, and the signal strength will decrease with distance. Different propagation models are available to predict the wave propagation. Large scale propagation models predict the mean signal strength as a function of the T_X-R_X separation. On the other hand, small scale propagation models predict the rapid fluctuations in the received signal over short distances (a few wavelengths). The free space propagation model predicts the signal strength at line of sight situations, where the T_X-R_X link is not obstructed. The well-known Friis formula categorizes this received signal as follow:

$$\frac{P_r}{Pt} = \frac{Gt.Gr}{L}\left(\frac{\lambda}{4\pi d}\right)^2 \qquad (5\text{-}1)$$

Where P_r, P_t, G_r, G_t are respectively the received power at a distance d, the transmitted power, the receiver antenna gain, and the transmitter antenna gain. λ is the wavelength, d is the T_X-R_X separation, and L is the system loss ($L \geq 1$).

The channel characterization is a process that studies the channel properties of a communication link. It is a study of the signal propagation from the transmitter to the receiver which represents the combined effect of different phenomena such as, scattering, fading, and

power decay with distance. Important channel parameters are of interest, namely the RMS delay spread, the path loss, the coherence bandwidth and the channel capacity.

This knowledge of the transmission channel in an underground mining environment is essential for the design of transmission systems that meets the need of miners. Following recent underground mining accidents, the development of a system dedicated to miner safety communications has become a primary need.

The characterization of the propagation channel consists in determining the parameters of the channel in order to understand the propagation mechanism or build a propagation model describing the behavior of the channel.

5.1) Large-scale channel characterization

Large-scale channel characterization consists of path loss (PL) and shadowing effect. Path loss is defined as the ratio of the received signal power to the transmit signal power [21].

In addition to free-space loss, the WBAN channel endures additional losses due to the shadowing obstacles, oxygen absorption, and rain attenuation. This poses a severe challenge in delivering a gigabit wireless transmission with reliable link margin.

Shadowing signifies the average signal power received over a large area (a few tens of wavelengths) due to the dynamic evolution of propagation paths, whereby new paths arise and old paths disappear [21]. Various measurement results reported in the literature have shown that the shadowing fading is log-normally distributed [48, 49]. Figure 5-1 presents a typical example of signal propagation in an indoor environment highlighting the types of fading [57]. Figure 5-2 shows the oxygen absorption and rain attenuation vs frequency.

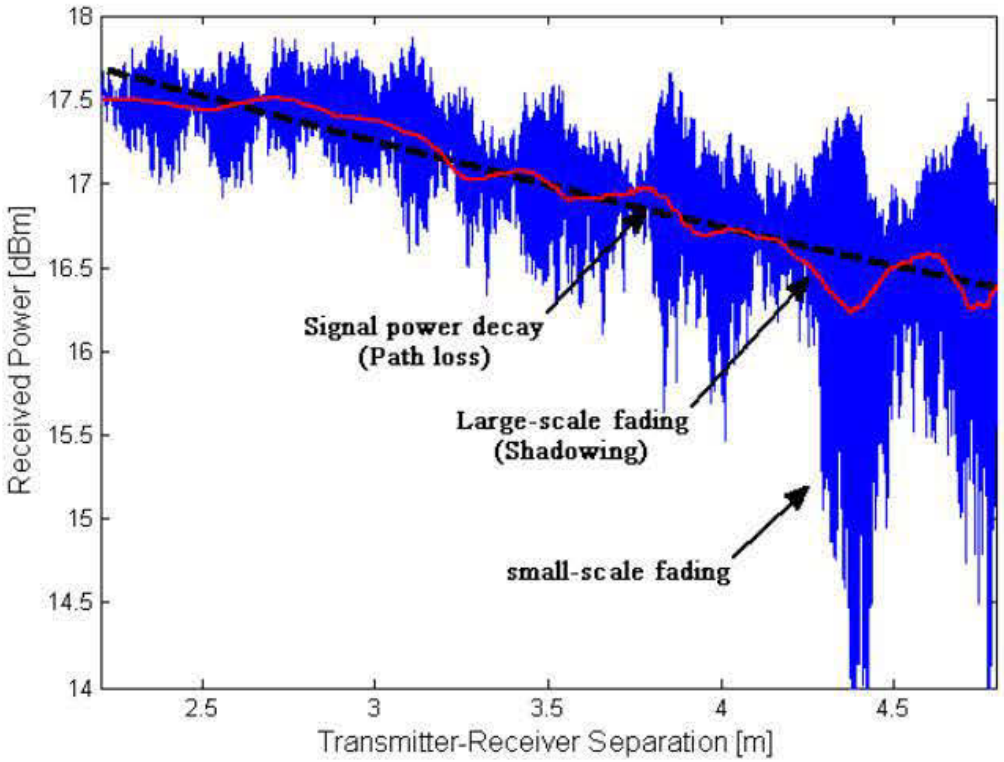

Figure 5- 1. Example of signal propagation in an indoor environment highlighting the types of fading [57].

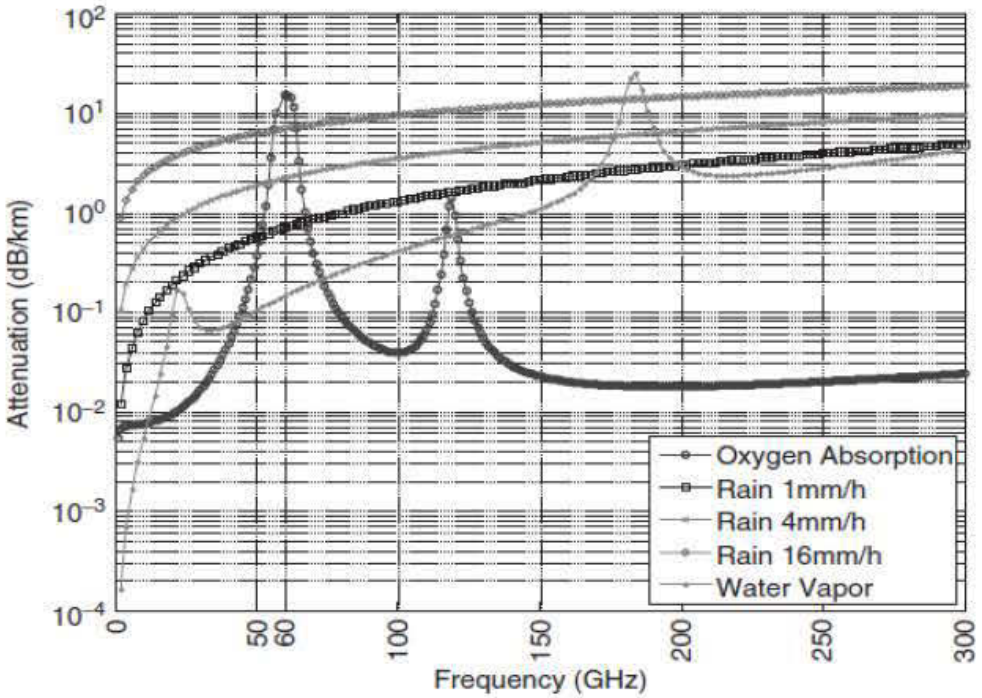

Figure 5- 2. Oxygen absorption and rain attenuation vs frequency [59]

5.2) Small-scale channel characterization

Small-scale channel characterization consists of small scale fading which is caused by the multipath signals that arrive at the receiver with random phases that add constructively or destructively. Small-scale fading causes rapid changes in signal amplitude over a small distance (less than 10 wavelengths). Over this small local area, the small-scale fading is approximately superimposed on the constant large-scale fading [21]. The multipath components cause the small scale fading effects that manifest in the following ways [21]:

- Steep fluctuations in the received signal through small distance intervals.
- Random frequency shifts due to the Doppler Effect on the different multipath signals.
- Time dispersion caused by the different multipath delays.

Small scale fading is especially of importance in urban area, tunnels, and galleries, where the direct line of sight is not always present, and the environment is rich in reflectors and scattering objects. Even in the presence of a LOS, the reflections from ground and other objects will cause multipath propagation. There are several physical factors which may affect the small scale fading.

- Multipath propagation caused by the presence of reflecting or scattering objects and in the channel. As a result, multiple replicas of the signal arrive at the receiver with different delays. The different multipath signals have random phases and amplitudes. When combining at the receiver, they result in random fluctuations in the received signal.
- The relative motion between the transmitter and the receiver will result in random frequency shifts of the multipath components due to the Doppler Effect.
- The movement of the surrounding objects will induce a time varying Doppler shifts in the multipath signals contributing to the small scale fading.
- The transmitted signal bandwidth will cause a distortion in the received signal if it is bigger that the multipath channel bandwidth.

5.3) WBAN channel characterization

The WBAN communication channels have many particularities that distinguish them from the regular RF system. In regular RF urban environments, the RF signal is mainly affected by the multipath and the shadow fading especially in a scattering environment or in NLOS situations. In the WBAN channels, the signal is also affected by the mere presence of the human body, which tends to damp the electromagnetic signal very strongly, especially at high frequencies. The choice of the antenna and their location on the body, and the choice of the operating frequency are therefore of outmost importance in order to achieve optimum performance. The on-body channel characterization at 2.45 GHz is performed for fourteen on-body channels in [50]. Furthermore, the link loss has been measured both in an anechoic chamber and in other surroundings, such as a laboratory; significant differences between the path loss of the different environments have been noticed in [51]. In off-body communication, human body-shadowing and time-varying fading may cause fluctuations in received signal characteristics, and hence affect the SNR and BER. This deterioration in the quality of the communications link can be mitigated through the use of spatial diversity at the receiver, which aims to remove deep fade and increase the mean received signal level [27].

5.4) Phenomenon affecting radio signal propagation inside a mine

The mining environment is a type of indoor environment, exhibiting many challenges to a wireless communication link. The characteristics of this environment are different from those of outdoor environments, due to the abundance of various factors affecting the radio propagation. These physical phenomena affecting radio wave encompass the following categories [52]:

- Fading which is the deviation of the attenuation affecting a signal over certain propagation media due to shadowing from obstacles or to multipath propagation.
- Diffraction which consists of the different phenomena that occur when a wave encounters an obstacle or a slit that has sharp irregularities (edges), resulting on the occurrence of secondary waves around the diffracting object.
- Reflection which is the change in direction of a wave at the interface of two media. Electromagnetic waves reflect easily and totally on the metallic mediums.

- Scattering which occurs in the presence of a large number of objects per unit of volume, with dimensions that are small compared to the signal's wavelength.
- Dispersion which is the phenomenon in which the phase velocity of a wave depends on its frequency.
- Waveguide effect which appears in a guided passage such as a tunnel or an underground gallery. In such an environment, the waves propagate along the direction of the guide.

The waves emitted during a radio communication generally undergo a combination of these phenomena. Therefore, the transmitted wave propagates along a multitude of paths. The received signal is the sum of all received beams along the different paths. This effect can cause destructive or constructive interference. It is also responsible for the observed fluctuations in the received signal, generally known as the fading. The parameters of a propagation channel are:

- Mitigation of power due to the distance, also known as the path loss.
- The amplitude variations due to obstacles, also known as the shadowing.
- The variations in amplitude and phase due to multipath.

Consequently, in order to mitigate the effects of the above mentioned phenomena, special attention should be taken in the design of antennas, their placement and their orientation. In the off-body communication , antennas should have radiation patterns directed away from the body, providing adequate coverage, and must be isolated from the body to avoid the effect of human body on the performance of the antenna [2]. In fact, the most important factor affecting the quality of the propagation in the off-body technology is shadowing. This is due to the movement of pedestrians clogging the radio off-body link and producing the effects of multipath. It has been found that the use of multiple antenna techniques (MIMO) reduces the effect of multi-paths on the off-body link [27].

In on-body environment, the link between the transmitter and receiver is affected by the movement of the body and on the antenna position on the body. Hence, it is of great importance to carefully choose the antenna type and properly locate it on the body. From among the difficulties associated with the on-body channel characterization is the non-

stationary state of the human body in normal activities due to different kind of movements; this affects the T_X-R_X link and makes LOS communication rare in most cases. Therefore, in order to characterize the radio wave propagation, one need to take into consideration the variable positioning of the terminals on the body and the dramatic changes in the geometry of the local environment. Moreover, one should bear in mind that the antenna performance, namely the input match and radiation pattern, is affected by the local geometry changes due to the movement. Hence, in order to enable a maximum channel capacity and minimum power consumption, one should consider the changes in the antenna positioning and the propagation loss during the design of the transceivers.

5.5) Channel parameters

5.5.1) Channel impulse response

A transmitted signal undergoes a filtering effect caused by the propagation channel prior to reaching the receiving antenna. The filtering nature of the channel is caused by the summation of the multiple arriving waves 'amplitudes and phases at any instant of time [21]. A static channel can be considered as a linear time invariant filter with an impulse response h(t) when it exhibits little or no changes over time. When it varies over time, due to the mobility of the receivers-transmitters environment, the equivalent filter will be varying over time.

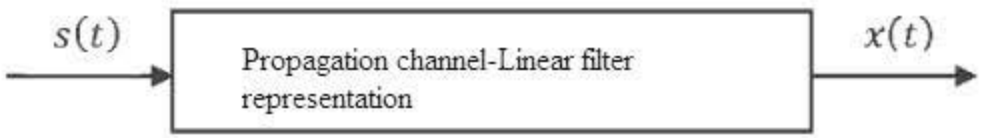

Figure 5- 3. Propagation channel linear filter representation [21]

In general, the transmitted and the received baseband signals are related by the well-known simple convolution:

$$x(t) = h(t) \otimes s(t) \qquad (5\text{-}2)$$

where $\mathbf{h(t)}$ and s(t) are respectively the impulse response of the propagation channel and the input signal.

The time invariant channel input response is described by the following formula [21]:

$$h(t) = \sum_{i=0}^{N} a_i e^{-j\theta_i}\, \delta(t - t_i) \qquad (5\text{-}3)$$

Where a_i and θ_i are the amplitude and phase of the i^{th} arriving multipath component; δ is the Kronecker delta function.

Actually, a short duration probing pulse is used instead of the unachievable delta function, during measurement.

In a mining environment, the propagation channel WBAN can be described by an impulse response h (t) where t denotes the time of the various paths of the transmitted signal. The WBAN is considered a quasi-static channel when the distance between the transmitting and receiving antennas at each measuring instant is fixed (the channel remains constant during the transmission). The impulse response is generally obtained by the inverse Fourier transform of the measured frequency response H (f) that is usually obtained using a vector network analyzer (VNA). As demonstrated in Figure 5-4, a frequency sweeper (used by the VNA) scans, in a discrete sense, a particular frequency band centered on the design frequency. The S-parameter test set transmits a known signal level at port one and monitors the signal level at port 2 for each frequency step. Hence, the complex frequency response, which is nothing more than the transmission coefficient S_{21} (f), is determined. An inverse discrete Fourier transform (IDFT) is then used to convert back to the time domain, hence giving a band limited version of the impulse response [21].

As for the MIMO impulse response, an inverse discrete Fourier transform is applied to the measured frequency-domain S_{21} sets of values allowing to determine the sub-channels' impulse responses; then, the MIMO channel impulse response is calculated as the arithmetic mean of all sub-channels' impulse responses, for each distance. Usually, the line of sight signal carries the highest power among the multipath received signals. In addition, it is expected that the LOS component is stronger for the smaller transmitter-receiver (Tx-Rx) separations, and gradually lessens in value as we increase this separation.

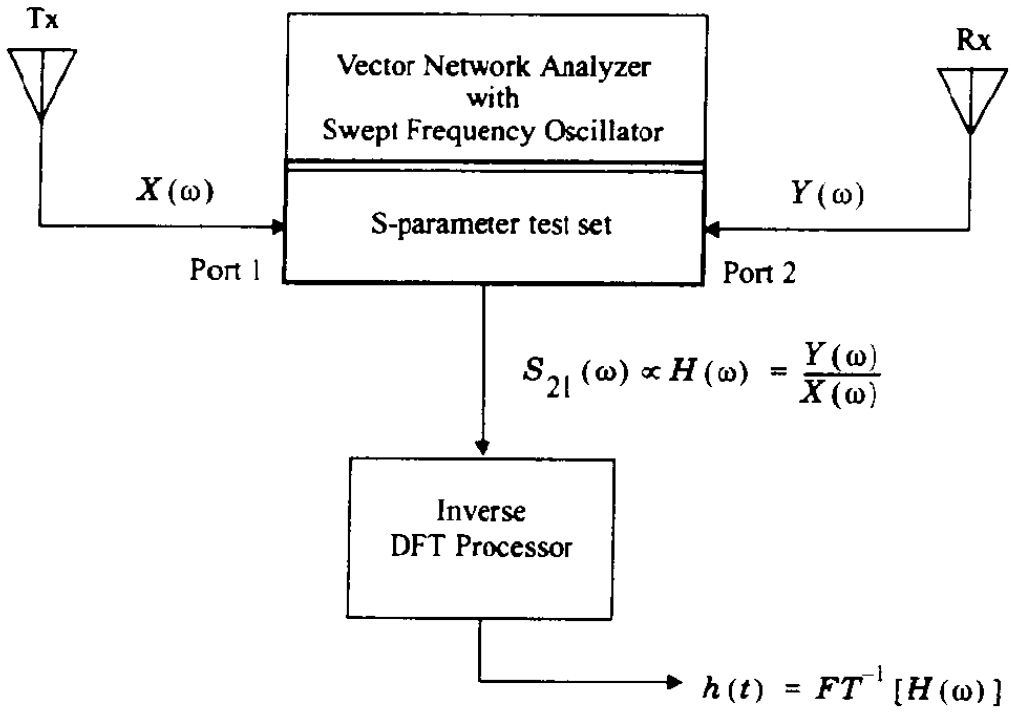

Figure 5- 4. Frequency domain channel impulse response measurement system [21]

The impulse response provides some valuable information about the channel. When plotted, it gives us a visual understanding of how strong are the multipath components. Furthermore, and with some minor processing, the impulse response is used to derive other important channel parameters such as the coherence bandwidth and the time delay spread, as it will be detailed in the following subsections, through the determination of the power delay profile. The power delay profile (PDP) is defined as a statistical average of the magnitude squared of the impulse response; the average concerns the different impulse responses at several random instants (close enough in time to insure the same channel conditions). The PDP is represented by the following formula [53]:

$$\text{PDP (t)} = \langle |h(t)|^2 \rangle \qquad (5\text{-}4)$$

In our measurements, the scattering parameters S_{21} are measured over a certain bandwidth and the Inverse Discrete Fourier Transformation (IDFT) is applied. Hence, the power delay profile (PDP) is estimated by averaging 6 static measurements taken at the different positions of the receive antenna. The random nature of the snap shots insures the

assumed statistically independent measurements. An example of the PDP is represented in Figure 5-5.

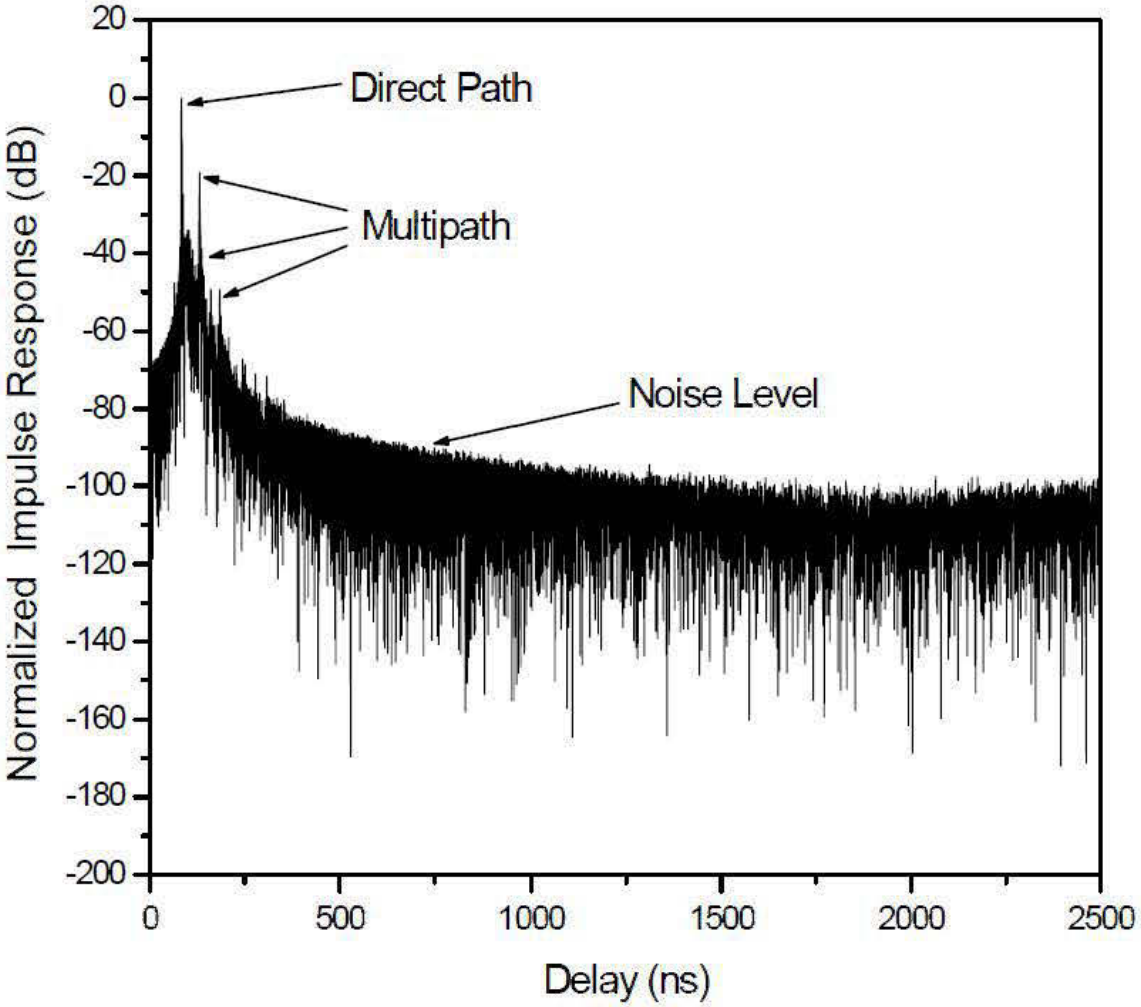

Figure 5- 5. An example of the PDP for radio propagation measurements inside a gold mine [53]

As a secondary usefulness, the impulse response is used to verify the measurements accuracy, by recalculating the distance where the LOS component is received using the old relation (Time × speed of the electromagnetic wave), and checking that this calculated distance is matching the intended distance during measurements.

5.5.2) Path loss

Path loss represents the reduction in power density (attenuation) of an electromagnetic wave as it propagates through space. It may be due to different effects, such as free-space loss, and oxygen/rain absorption.

The path loss is defined as the ratio of the transmitted power to the local average of the received power [19]; it is theoritically represented as follows:

$$PL_{dB} = 20Log_{10}(\xi\{G_{x,y,f}\}) \qquad (5\text{-}5)$$

Where $G_{x,y,f}$ is the spatial sub-channel path gain at a given frequency sample and a given snapshot and ξ is the expectation operator over all receiving antennas, transmitting antennas, frequencies, and snapshots [19].

For the SISO system, the path loss is obtained by averaging the path gains over the frequencies samples and the different snapshots [1], thus a special case of Eq. 5-5 which reduces it to the following expression:

$$PL(d(p)) = -20log_{10}\frac{1}{N_S N_f}\sum_{j=1}^{N_s}\sum_{n=1}^{N_f}\left|H_j^p(n)\right| \qquad (5\text{-}6)$$

Where $PL(d(p))$ denotes the path loss at a given position p (with T_X-Rx separation $d(p)$) and Ns and N_f are the total number of snapshots and frequency samples, respectively. $H_j^p(n)$ stands for the measured S_{21} parameter corresponding to the p^{th} position, the j^{th} snapshot, and the n^{th} frequency sample [1].

When expressed in terms of the Tx-Rx distance, the path loss can be modeled as [19]:

$$PL(d) = PL_{dB}(d_0) + 10.\alpha.log_{10}\left(\frac{d}{d_0}\right) + X \qquad (5\text{-}7)$$

where $PL_{dB}(d_0)$ is the mean path loss at the reference distance d_0 , d is the distance where the path loss is calculated, α is the path loss exponent which is determined using the least square linear regression analysis for instance, and X is a zero mean Gaussian variable (in dB) reproducing the shadowing effect.

5.5.3) RMS delay spread and Coherence bandwidth

The RMS delay spread is a parametter that quantifies the time dispersive properties of a multipath channel; it is determined using the following expression [21]:

$$\tau_{RMS} = \sqrt{\overline{\tau^2} - \bar{\tau}^2} \qquad (5\text{-}8)$$

Where the parameter $\bar{\tau}^2$ represents the second moment of the power delay profile (PDP) and $\overline{\tau}$ is the mean excess delay which can be formulated as follows:

$$\overline{\tau} = \frac{\sum_k a_k^2 t_k}{\sum_k a_k^2} = \frac{\sum_k p(t_k) t_k}{\sum_k p(t_k)} \qquad (5\text{-}9)$$

Where $p(t_k)$ denotes the power of the k^{th} path and t_k its corresponding delay; the delays are measured relative to the first detectable signal arriving at the receiver. The parameter a_k^2 is the overall time average of the squared magnitude of the channel impulse response. In indoor radio channels, typical values of the RMS delay spread are in the order of nanoseconds, while they are in the microseconds range for outdoor radio channels as depicted by table.5-1 [21].

Table 5- 1. Typical Measured Values of RMS Delay Spread [21]

Environment	Frequency (MHz)	RMS Delay Spread (σ_τ)	Notes	Reference
Urban	910	1300 ns avg. 600 ns st. dev. 3500 ns max.	New York City	[Cox75]
Urban	892	10-25 μs	Worst case San Francisco	[Rap90]
Suburban	910	200-310 ns	Averaged typical case	[Cox72]
Suburban	910	1960-2110 ns	Averaged extreme case	[Cox72]
Indoor	1500	10-50 ns 25 ns median	Office building	[Sal87]
Indoor	850	270 ns max.	Office building	[Dev90a]
Indoor	1900	70-94 ns avg. 1470 ns max.	Three San Francisco buildings	[Sei92a]

The coherence bandwidth is a channel parameter derived directly from the RMS delay spread. It is a well-known statistical measure of the range of frequencies over which the channel can be considered flat. In other words, it is the frequency range where two frequency components have a strong potential for amplitude correlation; hence in this range the different frequencies are affected in similar manner by the channel, in terms of amplitude [21]. The coherence bandwidth is an important parameter that is usually used to classify multipath fading into flat fading or frequency-selective fading depending on the channels' coherence bandwidth value relative to that of the transmitted signal. If the bandwidth of the signal is less than the coherence bandwidth of the channel, the channel's fading is said to be flat; in the opposite case, we are dealing with a frequency selective fading. The coherence bandwidth is calculated for a 50% correlation by adopting the following usual approximation [21].

$$B_C \simeq \frac{1}{5\tau_{RMS}} \qquad (5\text{-}10)$$

For a more strict definition, where the frequency correlation function is required to be above 0.9, then the coherence bandwidth is approximated by the following equation [21].

$$B_C \simeq \frac{1}{50\ \tau_{RMS}} \qquad (5\text{-}11)$$

In general, the coherence bandwidth and the RMS delay spread describe the time depressiveness of the channel, without giving any information about the time variation of the channel, which is sufficient and useful for static channels.

5.6) Different types of channel models

In order to investigate the performance of WBAN communication channels, channel modelling could be adopted. Different type of models exist to characterize the WBAN propagation channels. These models exhibits different advantages and a choice between models depends on the compromise between complexity and accuracy. While the purpose of

this thesis is limited to channel characterization, we chose to introduce briefly the channel modelling because of its importance in the signal propagation studies.

5.6.1) Deterministic modeling

There exist three types of deterministic modeling: the closed-form approach, empirical (based on measurement) approach, and ray tracing approach. An example of the closed-form approach is the two-path signal model [48], which is a simple model that allows theoretical analysis for different transmission schemes, but fails to give a realistic representation of the channel. The empirical approach uses channel parameters from the data collected in channel measurements conducted in a specific environment, to extract the channel parameters of this environment. This model is very accurate but requires a large amount of measurement data, which makes it complex and site specific. The ray tracing approach uses advanced electromagnetic theory and simulation tools (such as the uniform theory of diffraction and finite difference time domain) in developing the desired channel model. It requires the map of the site and defines the location of the different objects within the site. It is also environment-specific and very complex [48].

5.6.2) Stochastic modeling

Stochastic modeling is very popular and offers a good tradeoff between complexity and accuracy. Measurement data collected in a large array of locations within the environment under study allow developing stochastic models which provide a good statistical representation of the channel. This data allow the derivation of the probability density function (PDF) of the channel as well as the channel impulse response (CIR), which are needed for simulation purposes. One of the advantages of stochastic modeling is that it allows replicating various other different scenarios such as non-line-of-sight (NLOS) or other environments that share the same PDF by setting the channel parameters to the appropriate values.

5.7) Conclusion

This chapter explains the channel characterization, which consists in determining the parameters of the propagation channel in order to understand the propagation mechanism. It

details the stocastic approach used to studdy the signal propagation for a WBAN channel inside a mine galery. Large scale and small scale channel characterizations were described in terms of their related parametters. Moreover, the theoritical analysis of the channel impulse response, path loss, RMS delay spread, and coherence bandwidth is expounded in this chapter. Finally, different types of channel modelling have been described in this section to show the usefulness of the channel charcterization and modelling in predicting the behavior of a propagation channel. The theoritical background presented in this chapter and the previous chapters, is meant to enable the reader to understand the experimental results, for which the measurement environement and procedure are desribed in the next chapter.

CHAPTER 6

WBAN IN UNDERGROUND MINES

6.1) Measurement environment

Measurements campaigns were conducted in an underground gold mine. It is a former gold mine located near Val d'Or in Quebec (approximately 530 kilometers north-west of Montreal) and is managed by the Mining and Mineral Sciences Laboratories-Canadian Center for Minerals and Energy Technology (MMSL-CANMET). The gallery is located at the 40m underground level. It stretches over a length about 140 m with a width and height of about 3m. Photography of the underground gallery is shown in figure 6-1.

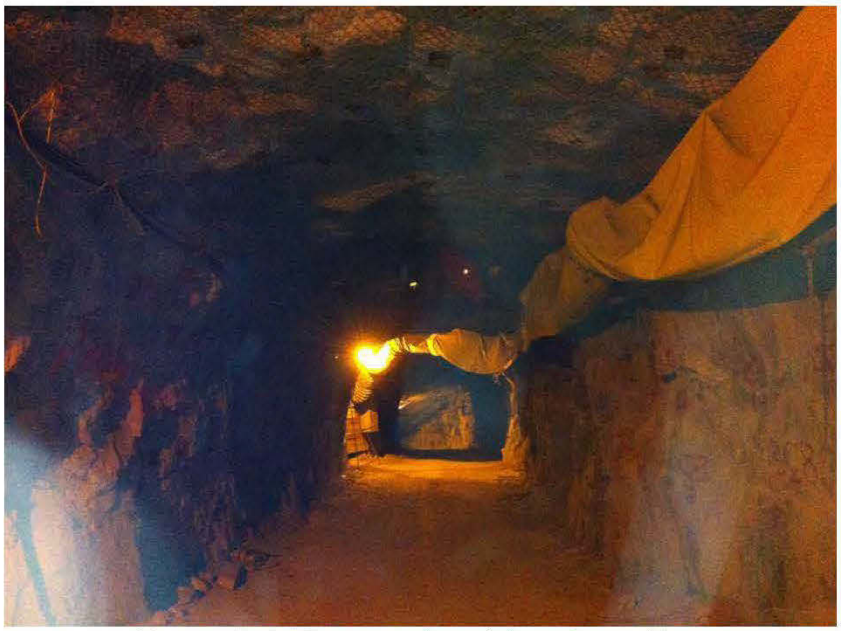

Figure 6- 1. Photography of the mine gallery

The environment consists mainly of very rough walls and uneven floor. Along these walls, cables and pipes are stretched (near the ceiling). The temperature is stable at 6 ° C, with a humidity level of nearly 100% throughout the year and water dripping through the

walls. There are some water puddles with different dimensions in a dusty environment. Metal rods and screens cover the ceiling of the gallery contributing to multipath phenomenon.

Figure 6-3 shows the 40 m level plan of the mine gallery. The site chosen allows a direct line of sight (LOS) communication in a well-controlled environment. It is an ideal environment to study the LOS and NLOS multipath propagation. Figure 6-2 and figure 6-3 provide a graphic representation of the measurement environment.

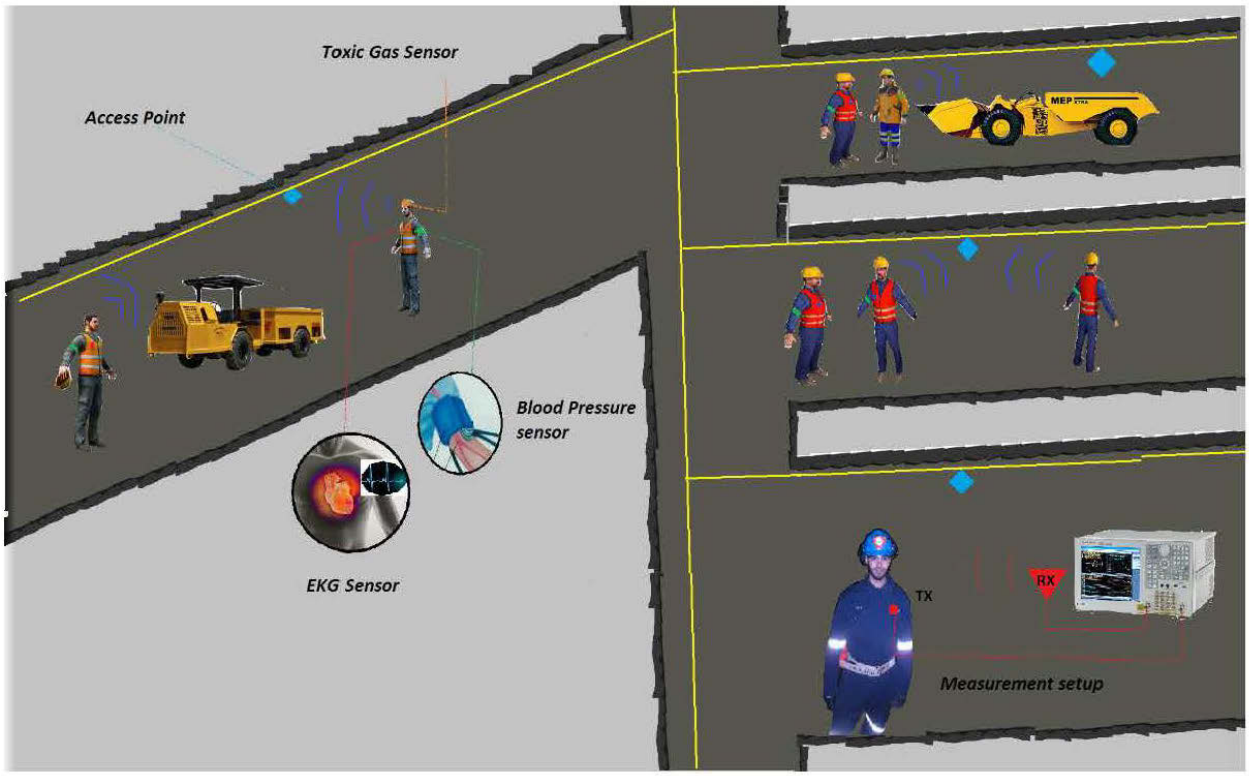

Figure 6- 2. Representation of the WBAN system in a mine environment

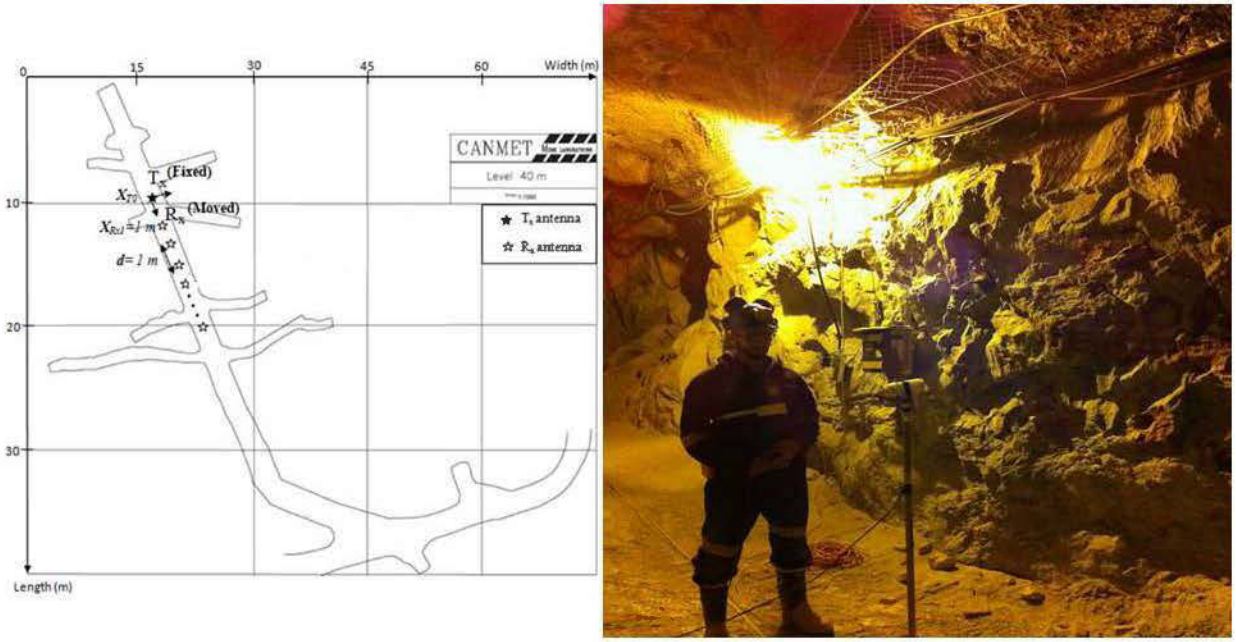

Figure 6- 3. Plan and photo capture of the measurement environment

6.2) Measurement campaign

The first step of the measurements' campaign is the system calibration. After the calibration, all the parameters were configured, namely the transmitting power, the Frequency range, and the nnmber of points as presented in table 6-1.

Table 6- 1. Measurement parameters

Equipment	**Parameter**	**Value**
VNA (of type Anritsu)		
	Frequency range	2GHz – 3GHz
	Number of points	6401
	Sweep time	Auto
	Calibration	Full-2-port (Tx power = -10 dBm)
Human body	Gender	Male
	Height	180cm
	Weight	75 kg
Antenna	Type	Monopole and patch
	Distance to body	5-10mm
	Orientation	Head to Head

The goal of the measurements is to investigate the small and the large scale variations in the fading signal. Large-scale channel characterization consists of path loss (PL) and shadowing effect, while the small-scale channel characterization consists of small scale fading which is caused by the multipath propagation. Two measurement scenario were considered.

6.2.1) On-body measurement procedure

In order to characterize the on-body SISO and MIMO channels in a mining environment at 2.45 GHz, three on-body channels were considered for the measurements. For each on-body channel, the transmitting antenna set (T_X) was placed at the left side position of the belt. The receiving antenna set (R_X) was placed alternatively at the right side of the chest (R_X 1), the right side of the head (R_X 2), and at the right wrist position (R_X 3), thus forming three on-body channels: belt-chest, belt-wrist, and belt- head as shown in figure 6-4. The transmitting antenna set was placed to point upward, and the receiving antenna set was pointing downward. The distance between the body and the antenna was kept at about 5-10 mm. The transmitting and receiving antennas were connected to the two ports of the vector network analyzer (VNA), after calibrating the VNA with the cables connected to it. The noise floor for the measurement was considered at -80dBm. Figure 6-5 shows the human test subject and antenna connections in the mine environment. The measurements were conducted in the CANMET gold mine near Val d'Or in Canada. A photo of the mine at the 40m level, where measurements were conducted, is shown in figure 6-3. This mine environment is very rough, dusty, and humid. The temperature is about 6° C throughout the year. The experiments were performed on a 1.80m, 75kg human male subject, in the 40m underground level of the mine. In order to study the significance of using MIMO on the results, a 2×2 MIMO monopole antenna set was used in addition to the SISO antenna set. During measurements, 6 data snapshots were collected, and the S_{21} parameter values are recorded for 6401 frequency samples around the center frequency of 2.45GHz at each scenario.

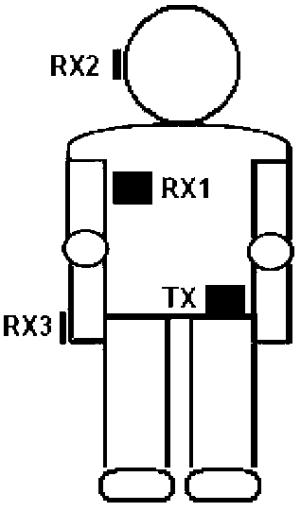

Figure 6- 4. Antenna positions for the on-body measurements

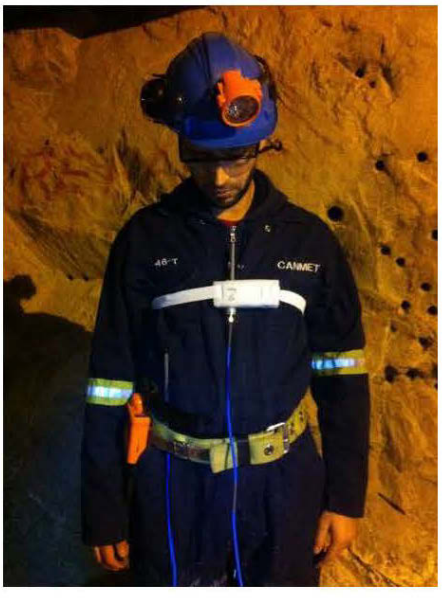

Figure 6- 5. On-body measurements test set up in a mine gallery

6.2.2) Off-body measurement procedure

In order to characterize the off-body SISO and MIMO channels propagation in this mine gallery at the 2.45 GHz band, the transmitting antennas were placed at a fixed position in the middle of the mine pathway (40m underground). The receiving antennas were placed on the right side of the chest of a 1.80m, 75kg male subject wearing a miner's outfit. Two types of MIMO antennas were used during the measurements, namely a 2×2 MIMO monopole

antenna set and a 2×2 MIMO patch antenna set. Both the transmit and the receive antenna elements are separated by a half wavelength distance, thus approximately 6 cm. During the measurements, 6 data snapshots were collected at each distance, from a distance of 1m through 5m away from the transmitter, as shown in figure 6-6 and figure 6-7. The transmitting and receiving antennas were connected to the two ports of the previously calibrated vector network analyzer (VNA). At each snapshot, the S_{21} values were recorded for 6401 frequency samples around the center frequency of 2.45 GHz, as indicated in Table 6-1. The noise floor for the measurements was considered at -90 dBm.

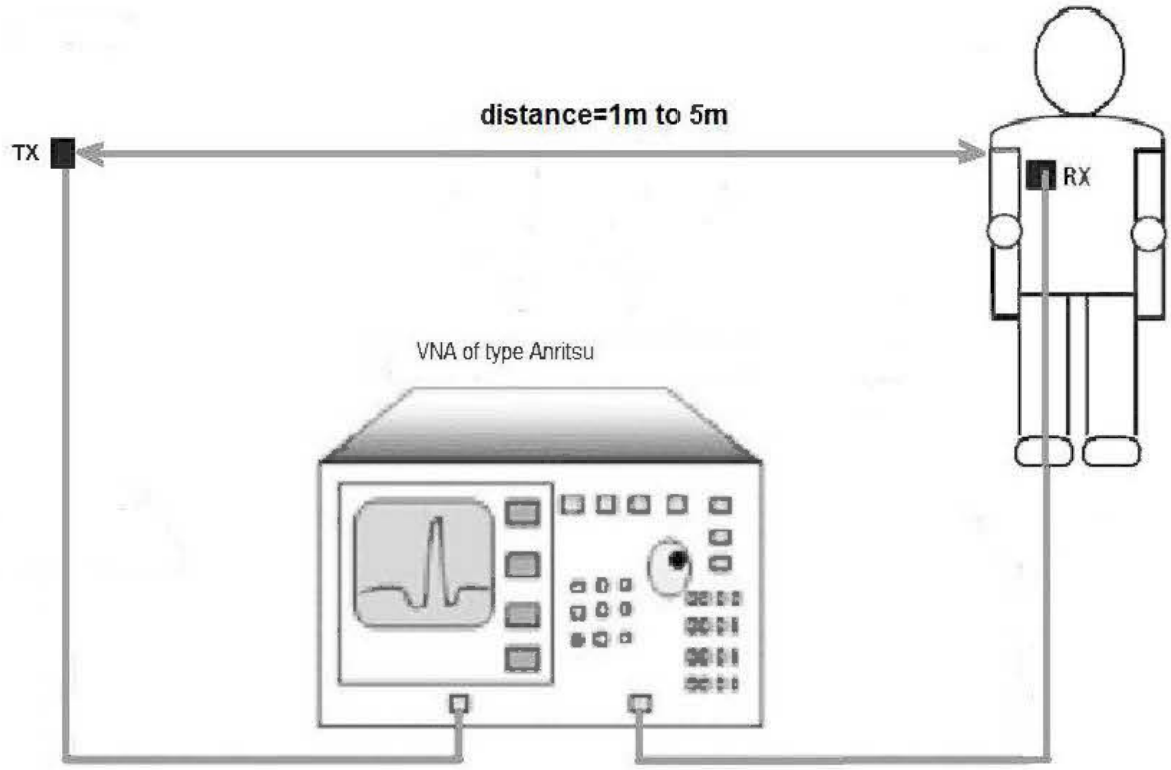

Figure 6- 6. Off-body measurement setup

Figure 6- 7. A photo of the off-body measurement setup

6.3) Measurement equipment

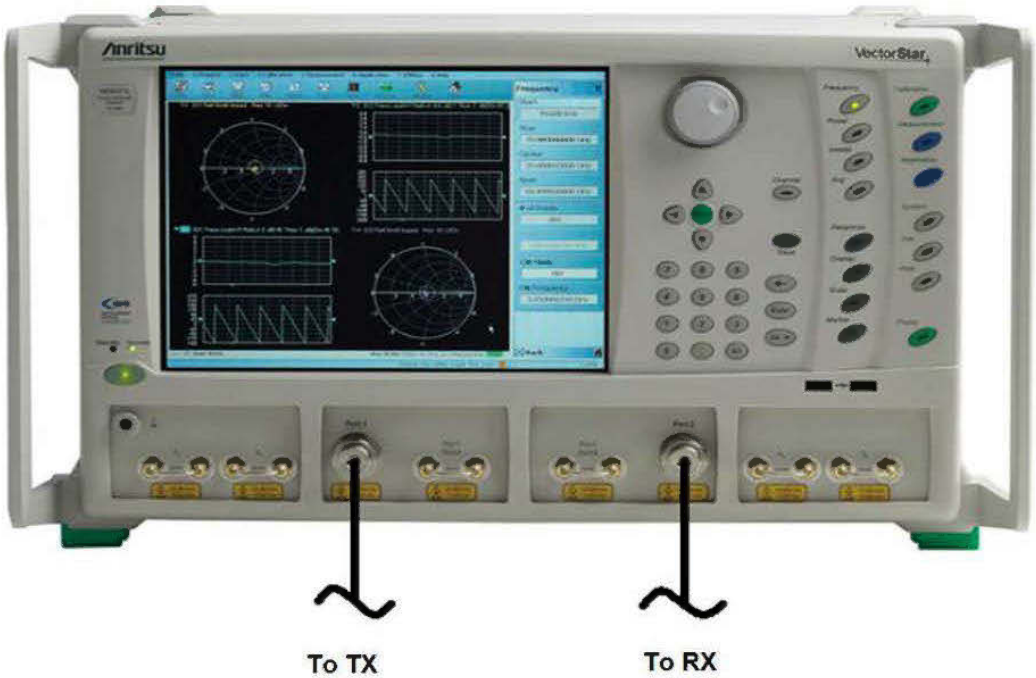

Figure 6- 8. A picture of the VNA used in on-body and off-body experiments

Figure 6- 9. Omni-directional and patch antenna used in our project

Table 6- 2. Measurements' equipment for on-body and off-body experiments

Equipment	Characteristics
Patch antenna	In lab manufactured antenna, 2.4 GHz, estimated 5dBi at 2.4GHz
Monopole antenna	RD2458-5, 3dBi at 2.4GHz
Cables	StormProduct true-blue serie - Attenuation–Nominal @ 2 GHz 0.110dB/ft
VNA	Anritsu MS4647A, 10 MHz to 70 GHz

Anritsu's MS4647A VNA is a 2 port VNA that offers the broadest coverage in a single 2 port instrument, 10 MHz to 70 GHz in a single instrument. It offers a system dynamic range at port 1 or 2 as follows of 122dB (0.01 to 2.5GHz) and 116dB (2.5 to 5GHz); the receiver compensation (at port 1 or 2) is 10dBm and the noise floor is -110dBm. The power range is +12 to -25dBm (for 0.01 to 2.5GHz), and +6 to -25dBm (for 2.5-5GHz), with a power accuracy of +/-1.5dB. The frequency resolution is 1Hz, with accuracy of 5×10^{-7} Hz/Hz. A typical 20µs/point is achieved with 25000 points in swept mode [54].

```
MS4647A
!12/3/2013.9:02:56.AM
!CHANNEL.1
!TR.MEASUREMENT
!RF.CORRECTION: FULL.TWO.PORT.CAL.PORT.1.2
!AVERAGING.OFF
!IF.BANDWIDTH: 1KHZ
!NUMBER.OF.TRACES: 2
!TRACE:          TRACE.1                    TRACE.2
!PARAMETER:      S21                        S21
!PORT:           PORT1                      PORT1
!GRAPH:          LOGMAG                     PHASE
!SMOOTHING:      OFF                        OFF
!TIMEDOMAIN:     OFF                        OFF
!SWEEPTYPE: FREQ.SWEEP(Linear)
PNT      FREQ1.GHZ        LOGMAG1 FREQ2.GHZ        PHASE2.DEG
1        2.000000000      -6.014098E+001  2.000000000      -140.9028000
2        2.000156250      -5.976746E+001  2.000156250      -143.0764000
3        2.000312500      -5.973798E+001  2.000312500      -142.1304000
4        2.000468750      -5.993771E+001  2.000468750      -141.4551000
5        2.000625000      -6.002834E+001  2.000625000      -143.2897000
6        2.000781250      -5.987485E+001  2.000781250      -143.2605000
7        2.000937500      -5.998438E+001  2.000937500      -144.5145000
8        2.001093750      -5.990554E+001  2.001093750      -142.5080000
9        2.001250000      -5.992855E+001  2.001250000      -144.3428000
10       2.001406250      -5.999758E+001  2.001406250      -143.1994000
11       2.001562500      -6.012484E+001  2.001562500      -144.5457000
12       2.001718750      -5.981043E+001  2.001718750      -144.4632000
13       2.001875000      -5.979582E+001  2.001875000      -147.3622000
14       2.002031250      -5.979286E+001  2.002031250      -146.6740000
15       2.002187500      -5.969761E+001  2.002187500      -146.9762000
16       2.002343750      -5.985317E+001  2.002343750      -146.1204000
17       2.002500000      -5.992878E+001  2.002500000      -146.1133000
18       2.002656250      -6.005640E+001  2.002656250      -147.1117000
19       2.002812500      -5.971186E+001  2.002812500      -149.0818000
20       2.002968750      -5.969112E+001  2.002968750      -146.9872000
21       2.003125000      -5.955787E+001  2.003125000      -147.0131000
22       2.003281250      -5.975012E+001  2.003281250      -148.3270000
23       2.003437500      -5.958792E+001  2.003437500      -148.6034000
24       2.003593750      -5.960225E+001  2.003593750      -149.3066000
25       2.003750000      -5.951204E+001  2.003750000      -149.1174000
26       2.003906250      -5.977505E+001  2.003906250      -150.2150000
27       2.004062500      -5.967335E+001  2.004062500      -150.0774000
28       2.004218750      -5.966980E+001  2.004218750      -148.6674000
29       2.004375000      -5.954507E+001  2.004375000      -150.8961000
30       2.004531250      -5.957541E+001  2.004531250      -150.8796000
31       2.004687500      -5.949991E+001  2.004687500      -150.8378000
32       2.004843750      -5.937963E+001  2.004843750      -153.2930000
33       2.005000000      -5.960226E+001  2.005000000      -150.5282000
34       2.005156250      -5.953682E+001  2.005156250      -151.5565000
35       2.005312500      -5.922464E+001  2.005312500      -151.4641000
36       2.005468750      -5.930595E+001  2.005468750      -151.5269000
37       2.005625000      -5.916336E+001  2.005625000      -152.6710000
38       2.005781250      -5.927577E+001  2.005781250      -153.0634000
39       2.005937500      -5.928174E+001  2.005937500      -152.4758000
40       2.006093750      -5.919128E+001  2.006093750      -153.8032000
41       2.006250000      -5.910254E+001  2.006250000      -154.4552000
42       2.006406250      -5.908219E+001  2.006406250      -154.1322000
43       2.006562500      -5.892239E+001  2.006562500      -153.6339000
44       2.006718750      -5.901337E+001  2.006718750      -156.4125000
45       2.006875000      -5.897984E+001  2.006875000      -154.5611000
46       2.007031250      -5.881155E+001  2.007031250      -156.0426000
47       2.007187500      -5.885757E+001  2.007187500      -156.7758000
48       2.007343750      -5.861242E+001  2.007343750      -156.1931000
49       2.007500000      -5.853476E+001  2.007500000      -156.0205000
50       2.007656250      -5.868357E+001  2.007656250      -155.0836000
51       2.007812500      -5.877993E+001  2.007812500      -158.3514000
52       2.007968750      -5.857158E+001  2.007968750      -158.0418000
53       2.008125000      -5.871248E+001  2.008125000      -158.8837000
54       2.008281250      -5.852905E+001  2.008281250      -159.0411000
55       2.008437500      -5.838123E+001  2.008437500      -159.7619000
56       2.008593750      -5.821304E+001  2.008593750      -160.0239000
57       2.008750000      -5.846538E+001  2.008750000      -161.3145000
58       2.008906250      -5.814125E+001  2.008906250      -162.7707000
59       2.009062500      -5.833948E+001  2.009062500      -161.5818000
```

Figure 6- 10. **Measurements output file of extension .TXT**

The VNA output file consists of the necessary data that are used in the post processing MATLAB codes in the signal propagation studies. The file contains a header with the date and time of the measurements, the intermediate frequency (IF) bandwidth and the parameters measured. The default number of columns is nine columns where the first column gives the discrete frequencies measured, and the subsequent columns denote the different magnitudes and phases of the S parameters. In our case, we modified the number of columns to only include the parameters of importance, namely the S_{21} parameter (magnitude and phase), as seen in figure 6-10.

The StormProduct true-blue series cables are designed for low loss, durability, general purpose test applications, and production testing. Their design covers frequencies from DC to 50 GHz, and is able to withstand temperature ranging from–54° C through +100° C. A low attenuation of 0.110dB/ft. at 2GHz is suitable for RF and microwave applications [54].

The RD2458-5 series of omnidirectional antennas offer a high-gain of 3 dB @ 2.4 GHz and are designed for indoor use. Their gain and pattern characteristics make it suitable for on-body and off-body applications [56].

The patch antenna is designed with a gain of about 5dBi and radiates toward the upper hemisphere [53].

6.4) Conclusion

In this chapter, the measurement environment and procedures are described for the on-body and off-body sets of experiments. The equipment used for this project have been described, in terms of their technical specifications. The experimental results and analysis are the subject of the following chapter.

CHAPTER 7

RESULTS AND ANALYSIS

7.1) On-body channel results

Three on-body channels (namely Belt-Head, Belt-Chest, and Belt-wrist) were characterized with the body at different postures corresponding to standard miners body states. The channel parameters were determined as described below.

7.1.1) Channel impulse response

By applying an inverse Fourier transform to the measured S_{21} values, the channel impulse response is determined for the SISO and MIMO antenna setups, for the on-body measurements inside a mine gallery. In the SISO configuration, figure 7-1 graphs show a stronger line of sight (LOS) component for the belt-chest channel (-53dBm) compared to the belt-wrist (-70dBm) and the belt head channel (-64dBm), with -10dBm transmitted power. This is due to the direct visibility provided by the belt-chest channel. The belt-chest channel is also the strongest for the MIMO configuration (-51dBm), as shown in figure 7-2.

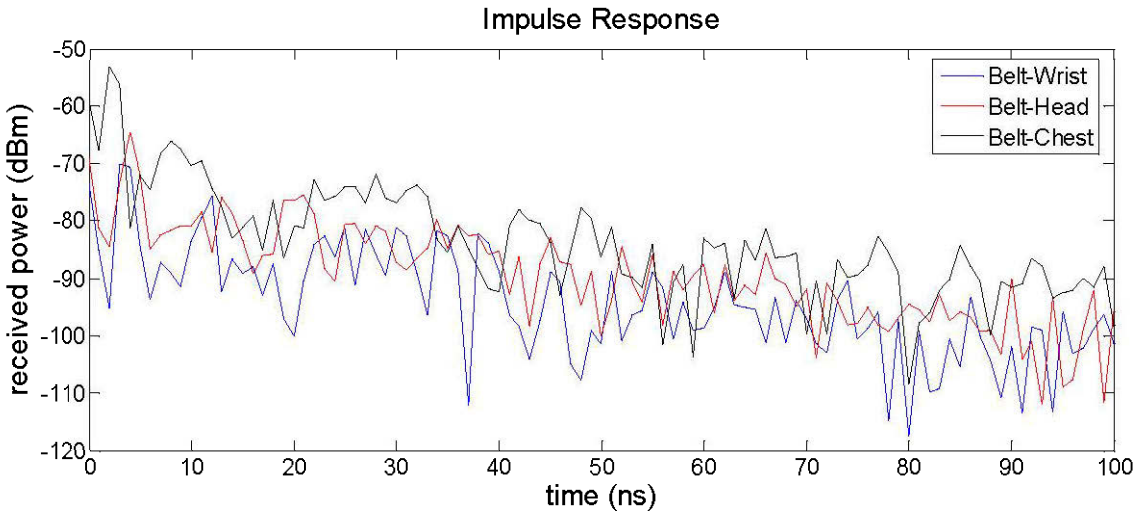

Figure 7- 1. Impulse responses for the three on-body SISO-M channels

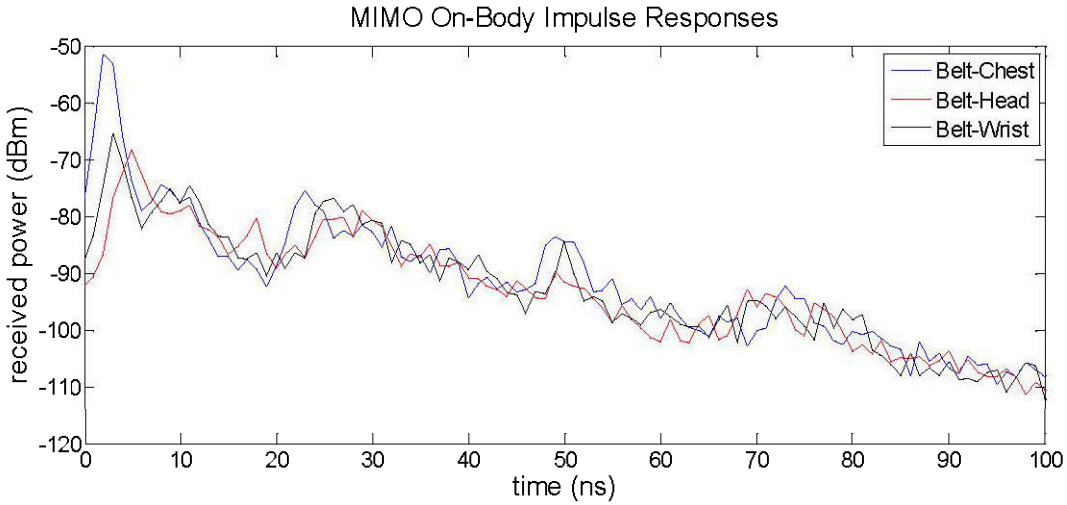

Figure 7- 2. Impulse responses for the three on-body MIMO-M channels

7.1.2) RMS delay spread and coherence bandwidth

The RMS delay spread quantifies the time dispersive properties of a multipath channel. It roughly characterizes the multipath propagation in the delay domain [53]. The RMS delay spread has been derived from the measured Power Delay Profile using (5-8) and (5-9).

The coherence bandwidth is inversely proportional to the RMS delay spread and measures statistically the range of frequencies over which the channel can be considered flat [21]. The coherence bandwidth is calculated using (5-10) or (5-11).

Results show values of the RMS delay spread for the SISO on-body channels that are in the order of 18.5-88 ns and the coherence bandwidth (at 50% correlation) in the range of 2.3-10.8 MHz as shown in table 7-1. For a MIMO on-body system, the results show the values of the RMS delay spread that are in the order of 18-90 ns and the values of the coherence bandwidth (at 50% correlation) in the range of 2.2-10.7 MHz. The MIMO on-body channel parameters are represented in table 7-2.

7.1.3) Channel capacity

The capacity of the SISO channel (plotted in Figure 7-3) is deduced from measurements using the Shannon formula (3-4). Similarly, the capacity of the MIMO channel (plotted in Figure 7-4) is deduced from the measurements using formula (3-5), described before.

The results show that the channel capacity for a channel with a strong line of sight (LOS) component (belt-chest channel) is higher than that of the other channels having less strong LOS component. This result is consistent both for the average channel capacity (in table 7-1 and table 7-2) and for the CDF plots at a certain probability level (figure 7-3 and figure 7-4). This is expected since a strong LOS component would result in a higher received power magnitude, and hence a higher SNR value. Detailed results for the average channel capacities of the SISO and MIMO channels are listed in table 7-1 and table 7-2; they show a clear improvement of the channel capacity due to the use of MIMO. This improvement is greatest for the channels exhibiting the highest LOS power; hence, the Belt-chest channel experienced an increase in capacity of 7.53 bps/Hz, due to the use of MIMO.

Table 7- 1. Parameters values for each SISO channel

Parameters	Measurement Channels For SISO On-Body		
	Belt-chest	Belt-head	Belt-wrist
Average channel Capacity (bps/Hz)	9.0779	5.4376	3.7368
Coherence bandwidth at 50% correlation (MHz)	10.800	3.4000	2.3000
Coherence bandwidth at 90% correlation (MHz)	1.0800	0.34000	0.23000
RMS delay spread (ns)	18.552	59.571	88.025

Table 7- 2. Parameters values for each MIMO channel

Parameters	Measurement Channels For MIMO On-Body		
	Belt-chest	Belt-head	Belt-wrist
Average channel Capacity (bps/Hz)	16.606	7.5565	7.7804
Coherence bandwidth at 50% correlation (MHz)	10.700	2.2000	2.7000
Coherence bandwidth at 90% correlation (MHz)	1.0700	0.22000	0.27000
RMS delay spread (ns)	18.721	89.397	73.703

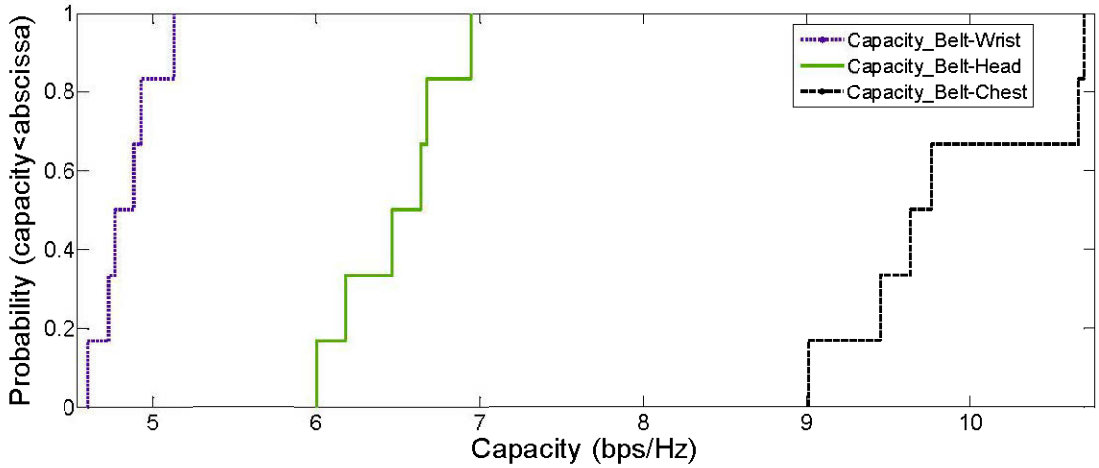

Figure 7- 3. SISO capacity CDFs for the three on-body channels.

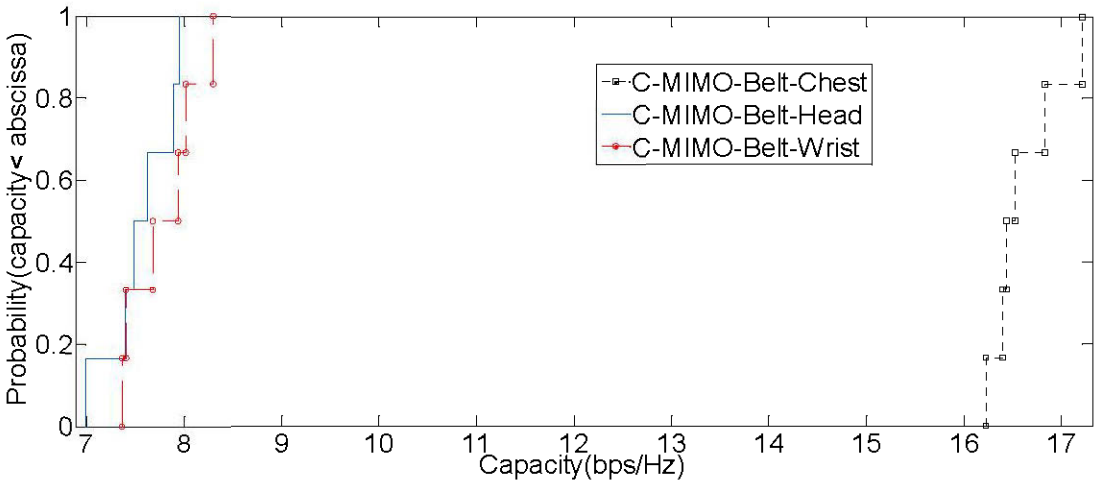

Figure 7- 4. MIMO capacity CDFs for the three on-body channels

7.1.4) Dynamic Channel parameters' Results

In addition to the measurement for a quasi-static channel, another campaign of measurements was performed with different sets of movements for the three channels (Belt-Head, Belt-Chest, and Belt-wrist). The activity sets, and the corresponding capacity results for the three channels are given in table 7-3. The results show that the movement of the human body has a minor effect on the capacity. This is clearly seen when comparing the results for a movement where the T_X-R_X length remains somewhat constant, to the average MIMO capacity of the corresponding Quasi-static channel. For instance, the capacity for a

belt-head channel when shaking the head from left to right is 4.3bps/Hz, which is close to 4.6bps/Hz that is found when shaking the head up-down. The length of the link, however, has a greater impingement upon the capacity values (with variations from the average capacity values of a static channel reaching up to 3 bps/Hz, when the length of the RX-TX link endures a big change during the movement).These results are expected, since the speed at which the receivers move with respect to the transmitter is negligible compared to the speed of light, making the observed frequency at the receiver (including the Doppler's effect), effectively the same as the emitted frequency. The channels are still considered effectively quasi-static. Table 7-3 represents the capacity values of the different on-body channels when the human subject undergoes certain typical body movements.

Table 7- 3. SISO capacity values corresponding to typical states of the human body

Belt-Head Postures	**Belt-Head Capacity (bps/Hz)**	**Belt-Chest Posture**	**Belt-Chest Capacity (bps/Hz)**	**Belt-wrist Posture**	**Belt-wrist Capacity (bps/Hz)**
Shaking head-left-right	4.3117	Moving arm-eating posture	9.9697	Moving arm-eating posture	7.2685
Shaking head-up-down	4.5742	Sitting down-typing posture	8.8971	Writing and typing	9.8955
Moving arm while standing	5.4722	Leaning down-while standing	8.4628	Lifting things from floor	9.0500
walking	3.8225	Leaning down-while siting	9.2291	Waving Bye-Bye	6.7058
Lifting things from floor - stand-sit movement	3.8018	Exercise-stand-sit	10.5443	Clapping	5.7947

7.2) Off-body channel results

7.2.1) Channel impulse response

An inverse Fourier transform was applied to the measured frequency-domain S_{21} sets of values in order to obtain the sub-channels' impulse responses; afterwards, the MIMO channel impulse response is calculated as the arithmetic mean of all sub-channels' impulse responses, for each distance. As expected, the line of sight signal carries the highest power among the multipath received signals. In addition, the LOS component is stronger for the smaller transmitter-receiver (Tx-Rx) separations, and gradually reduces in value as we increase this separation as seen in figure 7-5 and figure 7-6 for the case of SISO and MIMO configurations, respectively. Furthermore, the impulse response was used to verify the measurements accuracy, by recalculating the distance where the LOS component is received using the well-known relation (Time × speed of the electromagnetic wave), and comparing this calculated distance to the intended distance during measurements. In our case, we obtained a very close match with a distance error less than 20 %; the calculated distances come as follows: 1.2m, 2.4m, 3.3m, 4.2m, 5.4m for the monopole antenna and 1.2m, 2.1m, 3.3m, 4.2m, 5.4m for the patch antenna, which is very acceptable considering measurements errors, time resolution effect, and the fact that the real speed of the electromagnetic wave is a bit lower than the used speed of light.

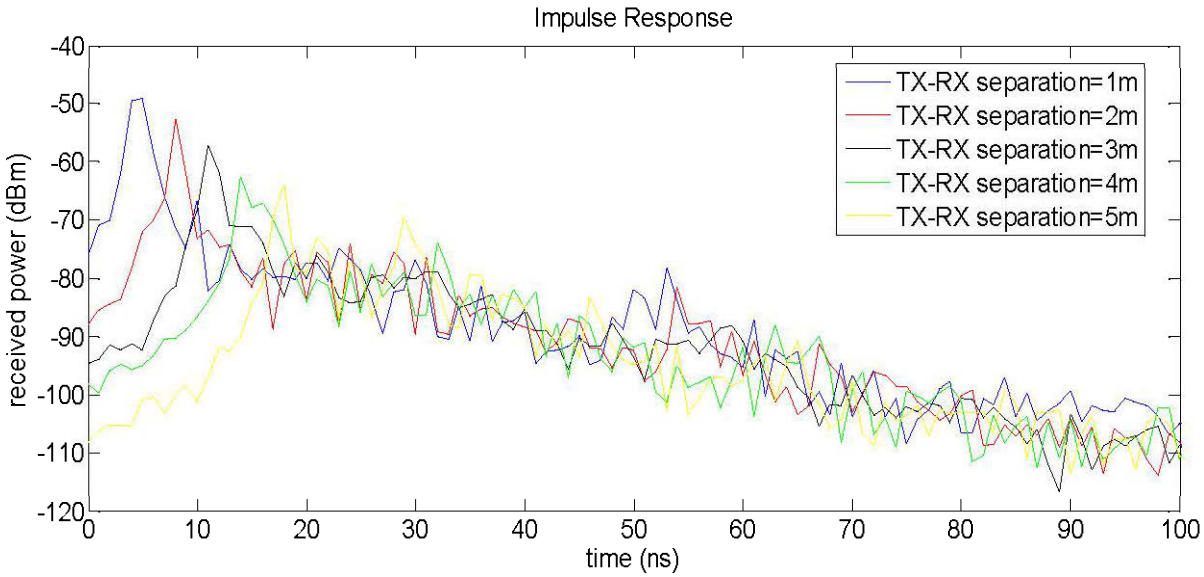

Figure 7- 5. Impulse responses for the different Tx-Rx separations in the case of SISO-monopole antennas in LOS situation.

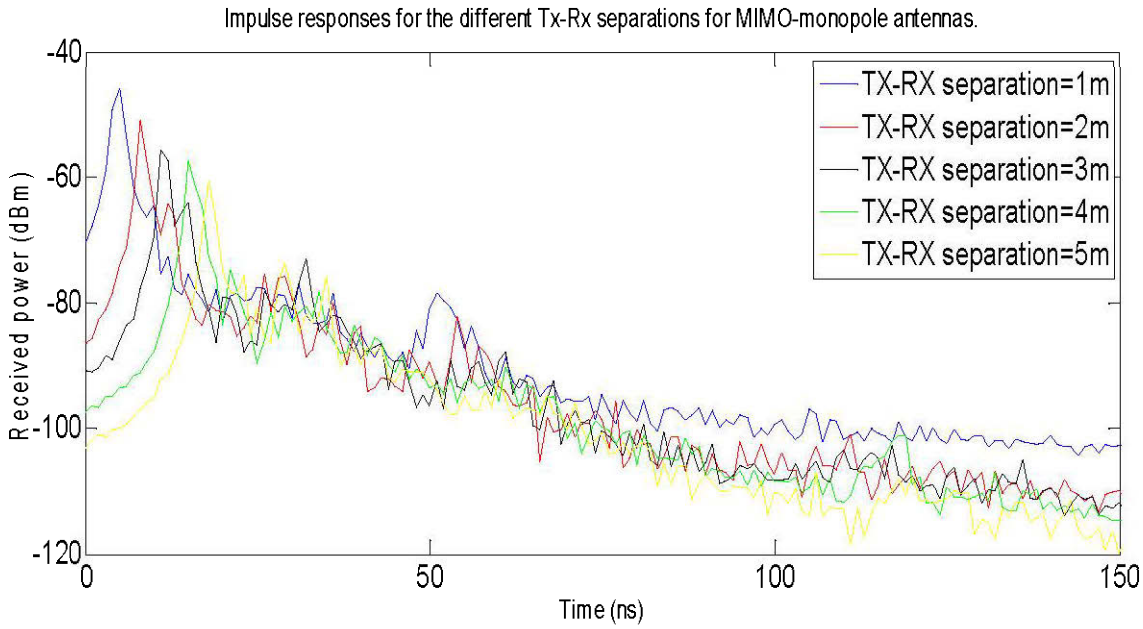

Figure 7- 6. Impulse responses vs. time for the different Tx-Rx separations in the case of MIMO-monopole antennas in LOS situation.

7.2.2) Path loss

The path loss was determined using equations (5-5) and (5-6) described before. The linear regression method was used to determine the path loss exponent in (5-7). The results show that the path loss increases with distance.

The path loss results obtained with monopole antennas in the case of SISO and MIMO systems are reported in figure 7-7 and figure 7-8, respectively.

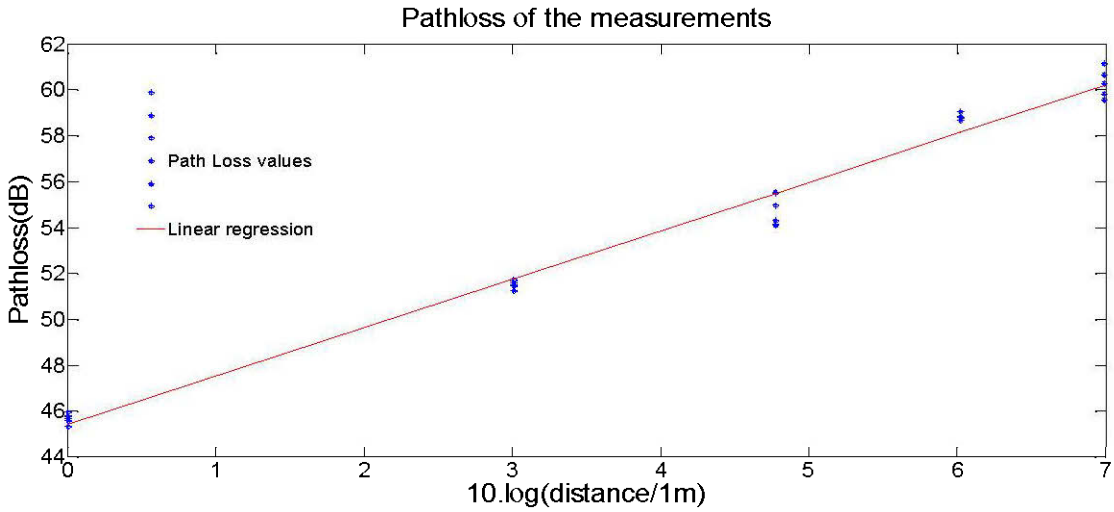

Figure 7- 7. Path Loss values and their linear regression for SISO-M at LOS configuration

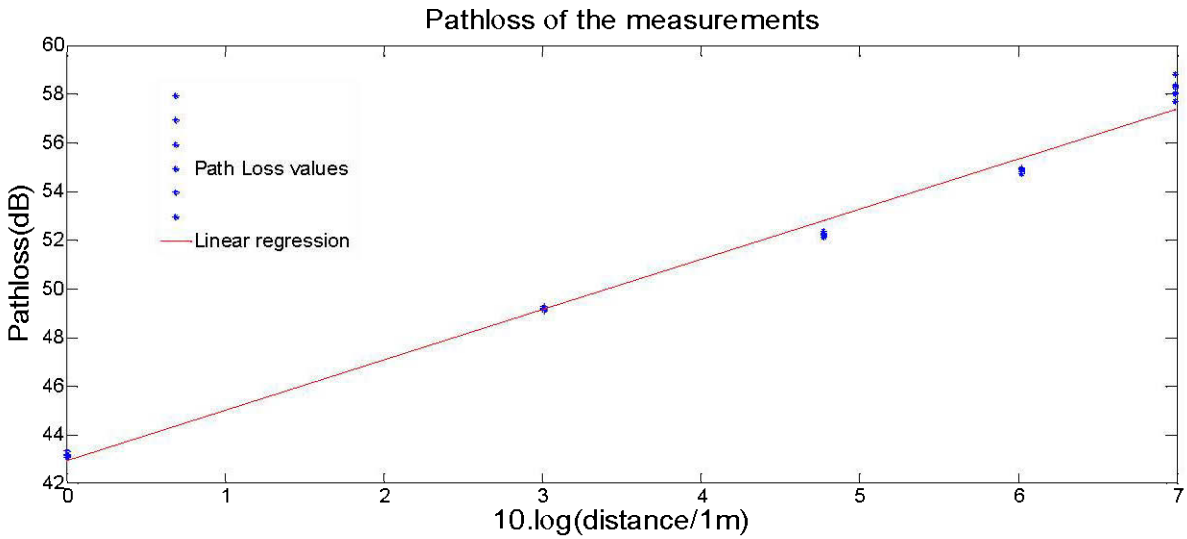

Figure 7- 8. Path Loss values and their linear regression for MIMO-M at LOS configuration

The above linear regression analysis shows that the path loss exponent α is close to the free-space path loss exponent (which is equal to 2) for the LOS configurations. Table 7-4 and table.7-5, which give some of the channel characterizing parameters, consolidate these results and show that, relative to LOS scenario, the path loss exponent decreases in SISO-NLOS configurations for both antenna types (monopole and patch). However, the path loss values are superior compared to LOS scenario due to the additive multipath effect in the presence of a human obstacle. This suggests that the signal is damped slower in SISO-NLOS due to constructive multipath power additions. The trend for the path loss exponent is not maintained in the case of MIMO topologies, while the path loss values are behaving in the same way. In general, the effect of the human obstruction is less severe than the obstruction caused by the mining machinery seen in [19].

Comparing the two types of antennas, the path loss exponent when using monopole antennas is generally lower than the path loss exponent when using patch antennas. This could be explained by the large beam width of the monopole antennas, leading to a more effective absorption of multipath energies, especially in NLOS situations.

7.2.3) RMS delay spread and coherence bandwidth

The RMS delay spread was determined using equations (5-8) and (5-9) described before. Similarly, the coherence bandwidth of the propagation channel is determined using equations (5-10) or (5-11), depending on the correlation level adopted.

Figure 7-9 and figure 7-10 represent the achieved RMS delay spread and coherence bandwidth vs. distance of the SISO-M and MIMO-M channels in the case of line of sight (LOS) conditions. It is clear that the RMS delay spread increases whereas the coherence bandwidth decreases with the increase of the distance. These figures show also RMS delay spread values that are between 15ns and 66 ns and coherence bandwidths in the range of 3-14 MHz for the SISO-M topology. The results for the MIMO-M topology show improvements in the RMS delay spread, with values varying from 13.6ns to 51 ns, and in the coherence bandwidths at 50% correlation level, with values spanning the range 3.9 MHz -14.7MHz. Other results for the NLOS conditions and for patch antennas are given in table 7-4 and table 7-5. From these tables, it is consolidated that for monopole antennas, the RMS delay spread is

decreased and the coherence bandwidth is increased by the use of MIMO systems in LOS conditions. With monopole antennas, the MIMO configuration brings the reverse effect in NLOS scenario, which means that the coherence bandwidth is decreased while the delay spread is increased. The reverse behavior is observed when the channel is measured using patch antennas. This could be explained by the higher directivity of patch antennas which reduces the number of perceived multipath components in NLOS scenario. The signal that crosses the human body obstacle is more weakened in the case of MIMO-P compared to MIMO-M, probably because MIMO-M system, due to its large beam width, allows to collect the LOS signal which power is higher than the multipath counterparts.

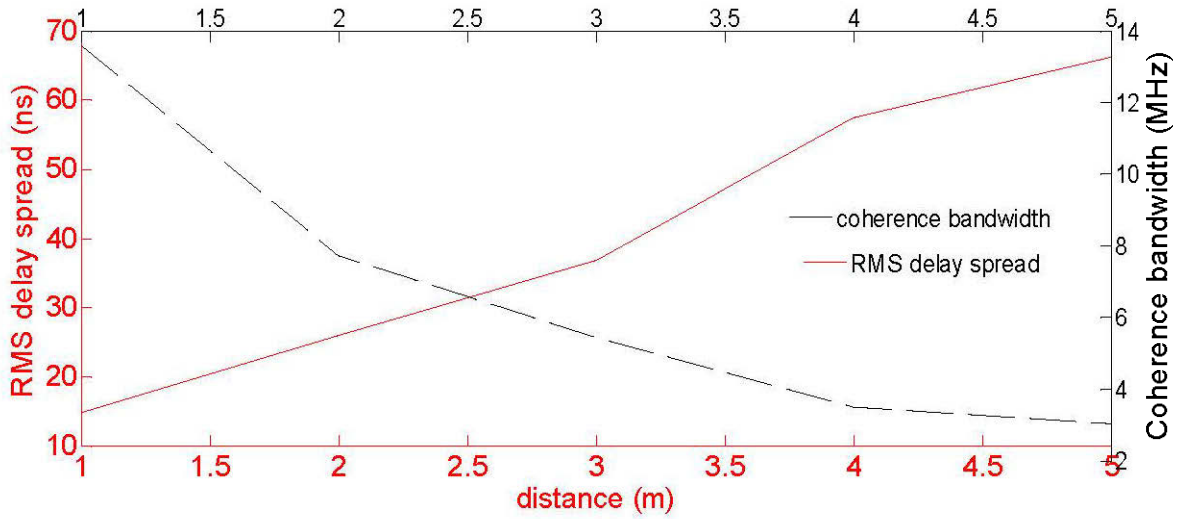

Figure 7- 9. SISO-M RMS delay spread and coherence bandwidth vs. distance

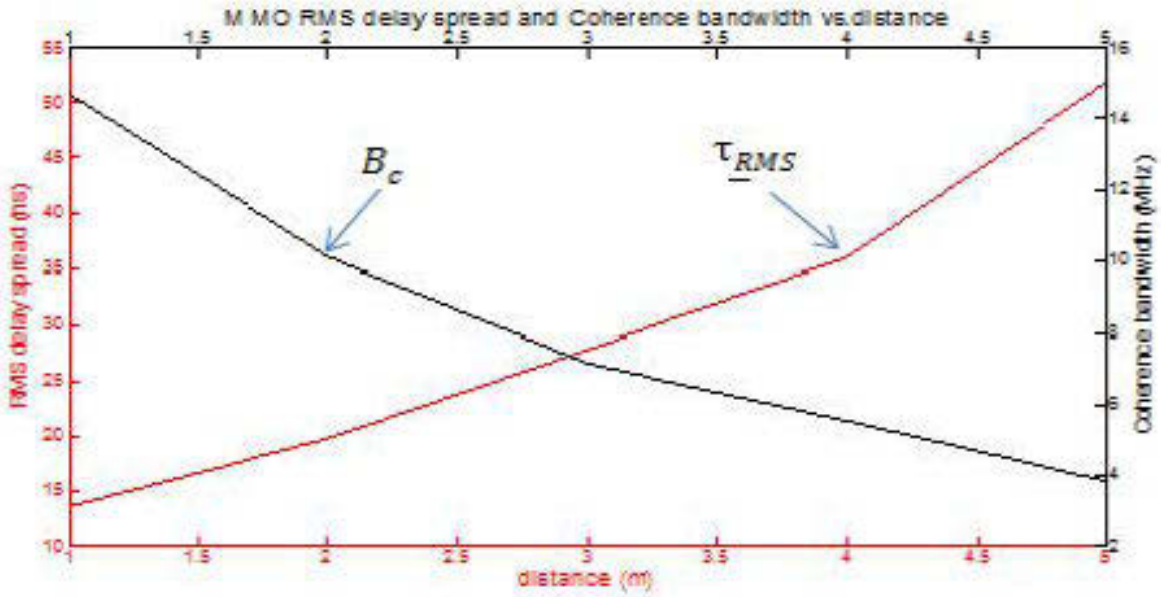

Figure 7- 10. MIMO-M RMS delayspread and coherence bandwidth vs. distance (bad quality)

7.2.4) Channel capacity

Channel ergodic capacity and its corresponding CDF are plotted in figure 7-11, 7-12, and 7-13 respectively, when using monopole antennas. The SISO capacityis calculated using the well-known Shannon formula (3-4) described above. Similarly, the capacity of the MIMO channel (plotted in Figure 7-13 for a monopole antenna) is deduced from the measurements using formula (3-5), described before.

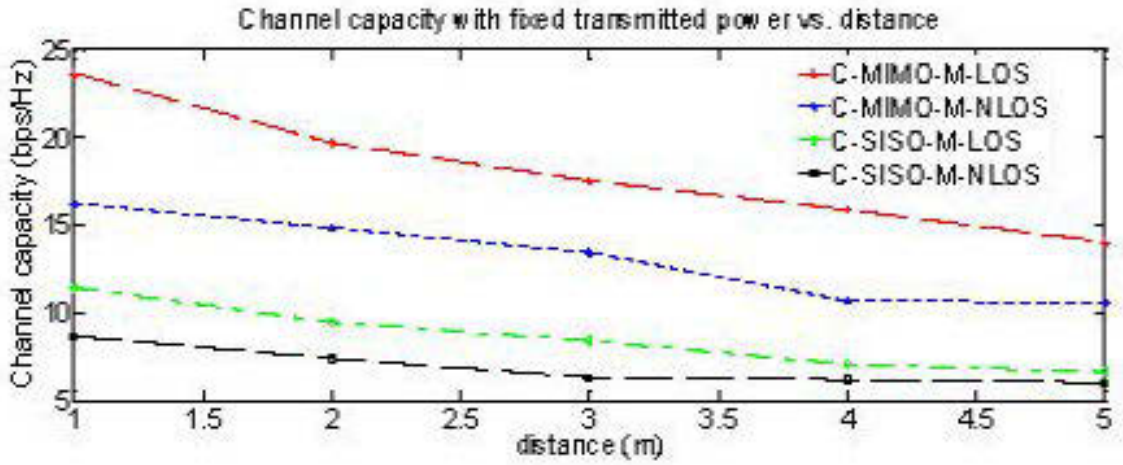

Figure 7- 11. MIMO-M and SISO-M average capacity vs. distance at LOS

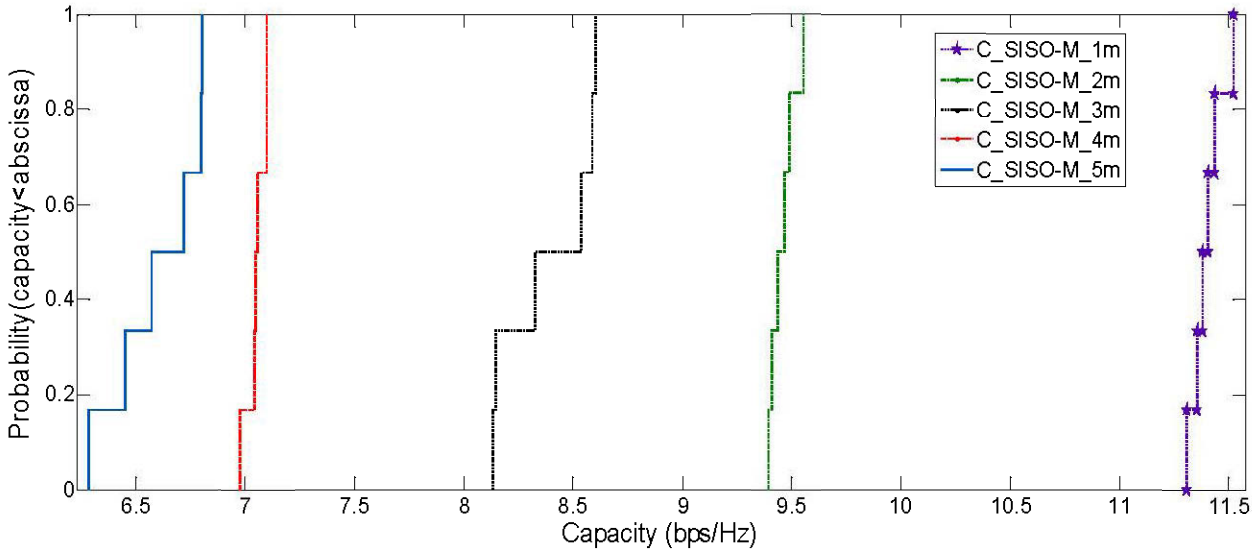

Figure 7- 12. SISO-M capacity CDFs for the five off-body channel 'distances

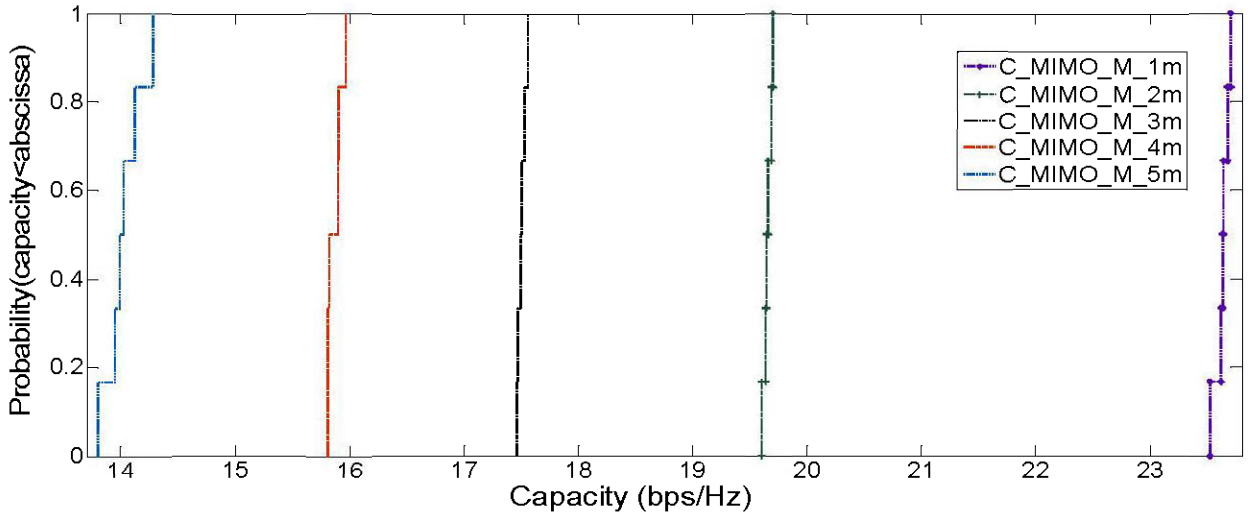

Figure 7- 13. MIMO-M capacity CDFs for the five off-body channel 'distances

As expected, the average capacity at a certain probability level decreases with distance. This is explained by the fact that the smaller distances correspond to higher received average powers and hence higher average SNRs which have a direct impact on the capacity as given in equations (3-4) and (3-5). Moreover, it is clear from figure 7-13 that the use of MIMO configuration offers an improvement in capacity compared to the SISO case. According to tables 7-4 and 7-5, this is valid for both monopole and patch antennas, in LOS and NLOS scenarios. This multiplexing gain provided by the MIMO technology is higher for the monopole antennas due to the fact that these antennas exhibit lower branch correlation.

Table 7- 4. Values of the different parameters of the off-body channel using monopole antennas

Configuration	**MIMO-M**		**SISO-M**	
Parameters	LOS	N-LOS	LOS	N-LOS
PL- exponent	2.0651	1.3104	2.1092	1.1775
PL (1m)	43.1746	55.9637	45.6828	54.1716
PL (2m)	49.1644	58.0329	51.5319	57.9437
PL (3m)	52.2357	60.3142	54.7589	61.6062
PL (4m)	54.8346	64.2788	58.7975	61.5095
PL (5m)	58.1974	64.4941	60.1628	61.9374
C_av_1m (bps/Hz)	23.6321	16.2338	11.4004	8.6683
C_av_2m (bps/Hz)	19.6613	14.8324	9.4589	7.3922
C_av_3m (bps/Hz)	17.5053	13.4182	8.3893	6.2876
C_av_4m (bps/Hz)	15.8673	10.6693	7.0542	6.1697
C_av_5m (bps/Hz)	14.0274	10.5772	6.6048	6.0236
$\tau_{RMS} - 1\text{m}$ (ns)	13.616	42.93	14.731	35.164
$\tau_{RMS} - 2\text{m}$ (ns)	19.834	52.79	25.927	55.725
$\tau_{RMS} - 3\text{m}$ (ns)	27.915	71.39	36.84	79.74
$\tau_{RMS} - 4\text{m}$ (ns)	35.97	110.9	57.436	82.567
$\tau_{RMS} - 5\text{m}$ (ns)	51.835	111.6	66.27	81.597
B_C_1m (MHz)	14.7	4.7	13.6	5.7
B_C_2m (MHz)	10.1	3.8	7.7	3.6
B_C_3m (MHz)	7.2	2.8	5.4	2.5
B_C_4m (MHz)	5.6	1.8	3.5	2.4
B_C_5m (MHz)	3.9	1.8	3	2.5

Table 7- 5. Values of the different parameters of the off-body channel using patch antennas

Configuration	**MIMO-P**		**SISO-P**	
Parameters	LOS	N-LOS	LOS	NLOS
PL- exponent	1.7293	2.0365	2.4813	1.2599
PL (1m)	49.4580	55.6565	45.3038	60.7453
PL (2m)	56.2576	63.8919	52.5457	68.9006
PL (3m)	58.9404	67.9946	56.6337	72.5153
PL (4m)	62.6108	71.8061	57.5081	67.7725
PL (5m)	60.1217	67.6193	64.4639	70.4411
C_av_1m (bps/Hz)	19.9922	18.5486	11.5263	6.4257
C_av_2m (bps/Hz)	15.5212	16.6418	9.1227	3.8273
C_av_3m (bps/Hz)	12.9498	9.0295	7.7689	2.7255
C_av_4m (bps/Hz)	10.9210	7.5237	7.4802	4.1612
C_av_5m (bps/Hz)	13.9749	8.8098	5.2016	3.3328
$\tau_{RMS} - 1\text{m}$ (ns)	42.92	49.1	24.38	69.48
$\tau_{RMS} - 2\text{m}$ (ns)	59.51	93.1	41.67	220.8
$\tau_{RMS} - 3\text{m}$ (ns)	80.35	198.9	60.13	356.2
$\tau_{RMS} - 4\text{m}$ (ns)	115.1	305.9	64.88	198.6
$\tau_{RMS} - 5\text{m}$ (ns)	72.81	201.1	141.5	279.4
B_C_1m (MHz)	4.7	4.1	8.2	2.9
B_C_2m (MHz)	3.4	2.1	3.5	0.9
B_C_3m (MHz)	2.5	1.0	4.8	0.6
B_C_4m (MHz)	1.7	0.7	2.2	1
B_C_5m (MHz)	2.7	1.0	2.5	0.7

7.3) Conclusion

In this chapter, we presented the results for two WBAN systems implemented in a mine gallery using SISO and MIMO antenna configurations. The first set of results consisted in the measured on-body channel parameters. It distinguished two types of channels, namely a static channel and a dynamic channel, where the human test subject undergoes typical movements. The second set of measurements describes the off-body channel performance through its measurement derived parameters, namely the channel impulse response, the path loss, the RMS delay spread as well as the channel capacity. The results clearly demonstrate the advantage of using MIMO configurations in both WBAN channels. A summary of the results is presented in the next concluding chapter.

CHAPTER 8

GENERAL CONCLUSION

8.1) Conclusion

In this project, the propagation channels on-body and off-body have been characterized in a mining environment. We considered two types of antennas, monopole (omnidirectional) and patch (directional) to study the effect of antenna directivity on the performance of the BAN-MIMO and BAN-SISO channels.

For the off-body channels, a 2×2 MIMO and SISO have been characterized in a mine gallery using monopole and patch antennas. Two scenarios (LOS and NLOS) were considered for measurements from 1m through 5m transmitter-receiver separations. It was observed that the path-loss increases with distance due to the decay in the received power, with a path loss exponent close to that of free space for most of the antenna configurations and types. In general, capacity decreases with the increase in distance due to the decrease in the average SNR. In NLOS situation, the multipath richness did not overcome the shadowing of the LOS component, and hence the capacity is lower than that of a corresponding LOS situation. For a certain transmit power, the presence of a strong LOS component imply a higher SNR at the receiver. In general, MIMO topologies provided a remarkable improvement in terms of capacity, coherence bandwidth, and time delay spread compared to the SISO topologies.

For the on-body channels, three SISO and MIMO channels have been characterized to investigate the significance of using MIMO for on-body applications in a mine gallery. The belt -chest channel is characterized by a strong LOS component. Hence, its channel capacities are higher than that of the belt-head and the belt-wrist channels for both MIMO and SISO topologies; this is explained by the higher received power, and hence the SNR, when a strong LOS component is present. Moreover, the capacity improvement using MIMO is significant for this channel due to the strong SNR and rich multipath. The other channels are characterized by a rich multipath phenomenon and weaker LOS component, which explains

the benefit of using MIMO for capacity amelioration (reaching an improvement of 3.36 bps/Hz for the Belt-wrist channel). When the human test subject undergoes certain typical body movements, the results were affected by the change in the TX-RX distances, due to the movement. The fact that the receiver is moving with respect to the transmitter, did not affect much the results when the T_X-R_X separation is somewhat constant. There is not a significant improvement in the RMS delay spread and coherence bandwidth due to the use of MIMO, because the richness of the multipaths tend to increase the RMS delay spread, while the strength of the LOS component tend to decrease it. Expectedly, the RMS delay spreads and coherence bandwidths of the Belt-chest channel is better than those of the belt-head and the belt-wrist on-body channels, for both the SISO and the MIMO topologies, suggesting that the Belt-chest channel could be considered more flat than the other two on-body channels.

The general conclusion that can be drawn from this master project is that the on-body and off-body channels can be used for communication in a mining environment, dedicated to the safety of miners. The BAN-MIMO systems are very promising to maximize the data rate and improve the capacity, even in the presence of practical problems such as the signal reflecting mining machinery and the interruption of a LOS link by other minors. The choice of the location of antennas must be made in such a way that maximizes the visibility between the transmitters and receivers in order to maximize the capacity.

In the future, we suggest to studdy the improvement in capacity using higher order MIMO-BAN systems (such as a 4×4 MIMO). We expect the higher order MIMO systems to offer better capacities, but with added complexity and TX/RX sizes; this trade-off between complexity and performance should be evaluated. Other types of diversity should be investigated, especially the polarization and pattern diversity schemes. It is also advisable to investigate other bands such as the 60 GHz channel, which would allow exploiting the high bandwidth offered in such a band. The high path loss associated with this band should be mitigated through the use of MIMO, in order to benefit from the small TX/RX dimensions while maintaining an acceptable performance.

References

[1] A.-M. Gao, Q. H. Xu, H.-L. Peng, W. Jiang, and Y. Jiang, " Performance Evaluation of UWB On-Body Communication Under Wimax Off-Body Emi Existence," Progress In Electromagnetics Research, Vol. 132, 479-498, 2012.

[2] Imdad Khan, "Diversity and MIMO for body-centric wireless communication channels", PhD thesis, University of Birmingham, September 2009.

[3] http://www.ieee802.org/15/pub/TG1.html

[4] http://www.zigbee.org/

[5] Carvey, P.P., "Technology for the Wireless Interconnection of Wearable Personal Electronic Accessories", IX VLSI Signal Processing Workshop,Oct. 30 – ,ov 1, 1996, pp. 13-22.

[6] M.R Kamarudin, Y.I.Nechayev, P.S.Hall, "Performance of Antennas in the On-body Environment", IEEE Antennas and Propagation Society International Symposium, 2005, 3-8 July 2005 pp. 475-478 vol. 3A.

[7] Y I Nechayev, P S Hall, C C Constantinou, Y Hao, A Alomainy, R Dubrovka, and C Parini, "Antennas and Propagation for On-Body Communication Systems", 11th Int. Symposium on Antenna Tech and Applied Electromagnetics – A,TEM, France, 2005.

[8] Y. I. Nechayev and P. S. Hall, "Multipath fading of on-body propagation channels," in Proc. IEEE Int. AP-S Symp.USNC/URSI National Radio Science Meeting, San Diego, CA, 2008, pp. 1–4.

[9] A.A. Serra, P. Nepa, G. Manara, P.S. Hall, "On the Performance Analysis of Diversity Techniques in Body-Centric Communication Systems," IET Seminar on Antenna and Propagation for Body-Centric Wireless Communications, London, UK, April 24, 2007, pp. 63-66.

[10] A.A. Serra, P. Nepa, G. Manara, and P.S. Hall, "Diversity Measurements for On-Body Communication Systems," IEEE Antennas and Wireless Propagation Letters, vol. 6 (1), pp. 361 – 363, 2007.

[11] S L. Cotton, W G. Scanlon, "Characterization and Modeling of the Indoor Radio Channel at 868 MHz for a Mobile Body-worn Wireless Personal Area Network", IEEE Antennas and Wireless Propagation Letters, vol.6, no., pp.51,55, 2007.

[12] S. L. Cotton, W. G. Scanlon, "Channel Characterization for Single- and Multiple-Antenna Wearable Systems Used for Indoor Body-to-Body Communications," Antennas and Propagation, IEEE Transactions on, Vol.57, No. 4, pp.980,990, April, 2009.

[13] Kvist, S.H.; Medina, P.F.; Thaysen, J.; Jakobsen, K.B., "On-body and off-body 2.45 GHz MIMO communications for hearing instrument applications," Antennas and Propagation (EuCAP), 2013 7th European Conference on , vol., no., pp.2595-2599, 8-12 April 2013

[14] Khan, I.; Hall, P.S., "Experimental Evaluation of MIMO Capacity and Correlation for Narrowband Body-Centric Wireless Channels," Antennas and Propagation, IEEE Transactions on , vol.58, no.1, pp.195-202, Jan. 2010.

[15] J. Molina Garcia Pardo, M. Lienard, A. Nasr, and P. Degauque, "On the possibility of interpreting field variations and polarization in arched tunnels using a model for propagation in rectangular or circular tunnels," Antennas and Propagation, IEEE Transactions on , vol.56, no.4, pp.1206,1211, April 2008

[16] Ben Mabrouk, I.; Talbi, L.; Nedil, M. "Performance Evaluation of a MIMO System in Underground Mine Gallery", Antennas and Wireless Propagation Letters, IEEE, On page(s): 830 - 833 Volume: 11, 2012

[17] J. Molina Garcia Pardo, J. V. Rodríguez, and L. Juan-Llacer, "Wideband measurements and characterization at 2.1 GHz while entering in a small tunnel," IEEE Trans. Veh. Technol., vol. 53, no. 6, pp. 1794–1799, Nov. 2004.

[18] M. Lienard, P. Degauque, J. Baudet, and D. Degardin, "Investigation on MIMO channels in subway tunnels," IEEE J. Sel. Areas Commun., vol. 21, no. 3, pp. 332–339, Apr. 2003.

[19] Ben Mabrouk, I.; Talbi, L.; Nedil, M.; Hettak, K. "MIMO-UWB Channel Characterization Within an Underground Mine Gallery", Antennas and Propagation, IEEE Transactions on, On page(s): 4866 - 4874 Volume: 60, Issue: 10, Oct. 2012

[20] Inanoglu, Hakan, "Multiple-Input Multiple-Output System Capacity: Antenna and Propagation Aspects," Antennas and Propagation Magazine, IEEE , vol.55, no.1, pp.253,273, Feb. 2013

[21] Rappaport, T.S.: 'Wireless communications: principle and practice' (Prentice Hall, 2001, 2nd edn)

[22] Wu, X. Y; Nechayev ,Y; Hall, P. S. "Antenna Design and Channel Measurements for On-Body Communications at 60 GHz", General Assembly and Scientific Symposium, 2011 XXXth URSI, On page(s): 1- 4, Issue: Aug. 2011

[23] Hou-Neng Wang; Li Ding; Zhi-Hong Guan and Jie Chen, "Limitations on minimum tracking energy for SISO plants," Control and Decision Conference, 2009. CCDC '09. Chinese, June 2009.

[24] Van Torre, P.; Vallozzi, L.; Rogier, H.; Moeneclaey, M.; Verhaevert, J. "Reliable MIMO communication between firefighters equipped with wearable antennas and a base station using space-time codes", Antennas and Propagation (EUCAP), Proceedings of the 5th European Conference on, On page(s): 2690 - 2694, Volume: Issue: , 11-15 April 2011

[25] I. Khan, P. S. Hall, A. A. Serra, A. R. Guraliuc, and P. Nepa, "Diversity Performance Analysis for On-Body Communication Channels at 2.45 GHz," IEEE Trans. Antennas Propag., vol. 57, no. 4, pp. 956-963, Apr. 2009.

[26] Alipour, S.; Parvaresh, F.; Ghajari, H.; Donald, F.K., "Propagation characteristics for a 60 GHz Wireless body area network (WBAN)," Military Communications Conference, 2010 - MILCOM 2010 , vol., no., pp.719,723, Oct. 31 2010-Nov. 3 2010.

[27] Ali, A.J.; Cotton, S.L.; Scanlon, W.G., "Spatial diversity for off-body communications in an indoor populated environment at 5.8 GHz," Antennas & Propagation Conference, 2009. LAPC 2009. Loughborough , vol., no., pp.641,644, 16-17 Nov. 2009

[28] Kelly, J.; Ford, L.; Langley, R., "Slotline structure for on/off-body communications at 2.45 GHz," Antennas and Propagation (EUCAP), Proceedings of the 5th European Conference on , vol., no., pp.525,529, 11-15 April 2011

[29] A Alomainy, "Antennas and Radio Propagation for Body-centric Wireless Networ", PhD Thesis, Queens Mary Uni, London, May 2007.

[30] T Salim, “Antennas for On-Body Communication Systems”, PhD thesis,University of Birmingham, September 2006.

[31] Chahat, N.; Zhadobov, M.; Sauleau, R., "Broadband Tissue-Equivalent Phantom for BAN Applications at Millimeter Waves," Microwave Theory and Techniques, IEEE Transactions on , vol.60, no.7, pp.2259,2266, July 2012

[32] L. T. B. M. M. N. a. N. K. I. B. Mabrouk, «Experimental characterization of a wireless MIMO channel at 2.4 GHz in underground mine gallery,» Progress In Electromagnetics Research Letters, vol. 29, pp. 97-106,, 2012.

[33] R G. Vaughan, J Bach Andersen, “Antenna Diversity in Mobile Communications”, IEEE transaction On Vehicular Technology, Vol. VT-36.N,o. 4 ,ov 1987.

[34] D Neirynck, C. Williams, A Nix, M. Beach, “Exploiting Multiple-Input Multiple-Output in the Personal Sphere”, IET Microwaves, Antennas and Propagations, Vol. 1,o. 6, Dec. 2007.

[35] Ghanem, K.; Hall, P.S. "Investigation of capacity of on-body channels using MIMO antennas", Antennas & Propagation Conference, 2009. LAPC 2009. Loughborough, On page(s): 161 - 164 .

[36] G. J. Foschini and M. J. Gans, “On limits of wireless communications in a fading environment when using multiple antennas,” Wireless Pers. Commun., vol. 6, pp. 311–335, Mar. 1998.

[37] G. J. Foschini, “Layered space–time architecture for wireless communication in a fading environment when using multielement antennas,” Bell Labs Tech. J., pp. 41–59, Autumn 1996.

[38] E. Telatar, “Capacity of multiantenna Gaussian channels,” AT&T Bell Laboratories, Tech. Memo., June 1995.

[39] G. Raleigh and J. M. Cioffi, “Spatial-temporal coding for wireless communications,” IEEE Trans. Commun., vol. 46, pp. 357–366, 1998.

[40] Bilel Mnasri, “ Caractérisation d'un canal de propagation souterrain en utilisant la technologie MIMO et le traitement dans le domaine angulaire”, Master thesis, Université du Québec en Abitibi-Témiscamingue, 2013.

[41] Lee, W. C Y, "Estimate of channel capacity in Rayleigh fading environment," Vehicular Technology, IEEE Transactions on , vol.39, no.3, pp.187,189, Aug 1990

[42] T. Svantesson and J. Wallace, “On signal strength and multipath richness in multi-input multi-output systems,” in Proc. IEEE Int. Conf. on Commun., May 2003, vol. 4, pp. 2683–2687.

[43] H. Carrasco, R. Feick, and H. Hristov, “Experimental evaluation of indoor MIMO channel capacity for compact arrays of planar inverted-F antennas,” Microw. Opt. Technol. Lett., vol. 49, no. 7, pp. 1754–1756,Jul. 2007.

[44] C B. Dietrich, Jr., K Dietze, J. R Nealy, and W L. Stutzman, “Spatial, Polarization, and Pattern Diversity for Wireless Handheld Terminals”, IEEE Transactions on Antennas and Propagation, Vol. 49, ,o. 9, September 2001.

[45] M. D. Turkmani, A. A. Arowojolu, P. A. Jefford, and C. J. Kellett “An Experimental Evaluation of the Performance of Two-Branch Space and Polarization Diversity Schemes at 1800 MHz”, IEEE Transactions on Vehicular Technology, Vol. 44, ,o. 2, May 1995.

[46] Per-Simon Kildal, K Rosengren, "Electromagnetic Analysis of Effective and Apparent Diversity Gain of Two Parallel Dipoles", IEEE Antennas and Wireless Propagation Letters, Vol. 2, 2003.

[47] Abbasi, Q.H.; Alomainy, A.; Yang Hao, "Ultra wideband antenna diversity techniques for on/off-body radio channel characterisation," Antenna Technology (iWAT), 2012 IEEE International Workshop on , vol., no., pp.209,212, 5-7 March 2012

[48] Yong, S.-k. (2010) Introduction to 60GHz, in 60 GHz Technology for Gbps WLAN and WPAN: From Theory to Practice (eds S.-K. (. Yong, P. Xia and A. Valdes-Garcia), John Wiley & Sons, Ltd, Chichester, UK. doi: 10.1002/9780470972946.ch1

[49] Anderson, C.R and Rappaport, T.S (2004) In-building wideband partition loss measurements at 2.5 and 60 GHz. IEEE Transactions on Wireless Communications, 3(3), 922–928.

[50] Y. I. Nechayev, P. S. Hall, C. C. Constantinou, Y. Hao, A. Alomainy, R. Dubrovka, C. G. Parini, "On-Body Path Gain Variations with Changing Posture and Antenna Position", the 2005 IEEE AP-S International Symposium on Antennas and Propagation and US,C/URSI ,ational Radio Science Meeting, Washington DC, USA on July 3-8, 2005.

[51] Hall, P.S.; Yang Hao; Nechayev, Y.I.; Alomainy, A.; Constantinou, C.C.; Parini, C.; Kamarudin, M.R.; Salim, T.Z.; Hee, D.T.M.; Dubrovka, R.; Owadally, A.S.; Wei Song; Serra, A.; Nepa, P.; Gallo, M.; Bozzetti, M., "Antennas and propagation for on-body communication systems," Antennas and Propagation Magazine, IEEE , vol.49, no.3, pp.41,58, June 2007

[52] S. Bug, C. Wengerter, I. Gaspard, R. Jakoby: "WSSUS-Channel Models for Broadband Mobile Communication Systems". Proceedings of the Vehicular Technology Conference, Vol.2, 894 -898, 2002.

[53] Ben Mabrouk, "Caractérisation d'un Canal Minier Souterrain Utilisant les Techniques MIMO", PhD thesis, Université du Québec en Outaouais, 2012.

[54] http://www.anritsu.com/en-GB/Promotions/VstarB/Lit-packs/11410-00432E_VectorStar_MS4640B_TDS.pdf

[55] http://www.teledynestorm.com/microwave/mw_cablefxgp.asp?div=mw&cg=421

[56] http://lairdtech.thomasnet.com/item/ice-provider-wisp-base-station-and-client-antennas/rubber-duck/rd2458-5-1

[57] Mohamad Ghaddar, "Experimental Characterization and Modeling of Short-Range Wireless Propagation Channels in the Unlicensed 60 GHz Band", PhD thesis, Université du Québec en Outaouais, 2012.

[58] Khan, Mohammad Monirujjaman; Abbasi, Q.H.; Alomainy, A.; Yang Hao; Parini, C., "Ultra wideband off-body radio channel characterisation and modelling for healthcare applications," Wireless Telecommunications Symposium (WTS), 2012 , vol., no., pp.1,5, 18-20 April 2012

[59] Yong, S.-k. (2010) Introduction to 60GHz, in 60 GHz Technology for Gbps WLAN and WPAN: From Theory to Practice (eds S.-K. (. Yong, P. Xia and A. Valdes-Garcia), John Wiley & Sons, Ltd, Chichester, UK.

ANNEXE A: Published articles

Performance Evaluation of a SISO On-Body System in a Mine Evironment

Moulay El Azhari, Mourad Nedil, Ismail Ben Mabrouk
Underground communications research laboratory
UQAT, Val d'Or, Canada

Abstract: In this paper, the on-body performance of a single-input single-output (SISO) system was evaluated. Measurement campaigns using Monopole antennas have been taken in a gold mine. Three on-body channels were characterized in terms of the channel impulse response, RMS delay spread, coherence bandwidth, and channel capacity. The variation of these parameters in the different measurement scenarios was discussed.

Keywords: SISO, on-body channel, channel capacity, frequency response,impulse response.

INTRODUCTION

Body area network (BAN) is a growing communication technology that found many applications in personal health care, entertainment, military, firefighting and many other fields [1]. Various articles in the literature deal with on body communication systems, for patients' vital signs monitoring application [2].

This technology could acquire valuable applications in the mining environment because of its simplicity and its ability to guaranty information delivery and environment conditions monitoring. In fact, miners are subject to a number of potential health hazards in their normal daily work. It is therefore of outmost importance to ensure that workers are not exposed to health hazards at levels likely to result in adverse health effects by **recognizing, assessing** and **controlling** all potentially hazardous agents and factors (such as harmful gases) that the miners are potentially exposed to at work. A reliable BAN communication system would be both cost effective and simple to use in a mine gallery.

If a BAN system, based on electronic sensors, were to be deployed for miners' vital signs and in-mine environmental conditions monitoring, it would allow a fast detection of potential problem (such as an in-mine fire) and hence improve the miners' safety.

In this paper, the performance of a single-input single-output (SISO) BAN system, in a mine gallery, is evaluated at the 2.45 GHz ISM band. Three on-body channels (Belt-Head, Belt-Chest, and Belt-wrist) were characterized with the body at a standstill posture. The channel capacity was derived from the measurements (using the Shannon equation in [3]) and compared for the three on-body channels. The RMS delay spread, and the coherence bandwidth were also derived (using equations in [4]) and compared for the different measurement scenarios. The proposed measurement scenarios are briefly discussed in section II and the results are provided in section III.

MEASUREMENT PROCEDURE

To characterize the on-body SISO channels in a mining environment at 2.45 GHz, three on-body channels were considered for the measurements. For each on-body channel, the transmitting monopole antenna was placed at the left side position of the belt. The receiving antenna was placed alternatively at the right side of the chest, the right side of the head, and at the right wrist position, thus forming three on-body channels: belt-chest, belt wrist, and belt head as shown in Fig.1. The transmitting antenna was placed to point upward, and the receive antenna was pointing downward. The distance between the body and the antenna was kept at about 5-10 mm. The transmitting and receiving antennas were connected to the two ports of the vector network analyzer (VNA), after calibrating the VNA with the cables connected to it. The noise floor for the measurement was considered at -80dBm.

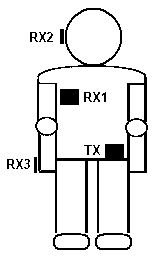

Antenna positions

RESULTS

Channel impulse response

The channel impulse response is determined from the measured S_{21} values by applying an inverse Fourier transform. The graphs show a stronger line of sight (LOS) component for the belt-chest channel (-53dBm) compared to the belt-wrist (-

70dBm) and the belt head channel (-64dBm), with -10dBm transmitted power.

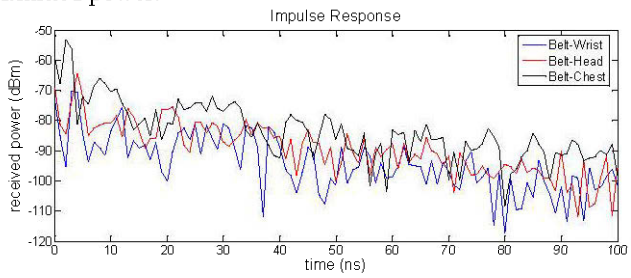

Figure 1. Impulse responses for the three on-body channels.

RMS delay spread and Coherence bandwidth

The RMS delay spread was derived from the measurements using (1); it quantifies the time dispersive properties of a multipath channel [4].

$$\tau_{RMS} = \sqrt{\overline{\tau^2} - \overline{\tau}^2} \qquad (1)$$

The parameter $\overline{\tau}$ represents the mean excess delay and $\overline{\tau}^2$ is the second moment of the power delay profile (PDP) [4].

$$\overline{\tau} = \frac{\sum_k a_k^2 t_k}{\sum_k a_k^2} = \frac{\sum_k p(t_k) t_k}{\sum_k p(t_k)} \qquad (2)$$

The parameter $p(t_k)$ is the power of the k^{th} path and t_k is its delay. The parameter a_k^2 is the overall time average of the magnitude squared of the impulse response (6 measurements are averaged).

Coherence bandwidth is inversely proportional to the RMS delay spread and measures statistically the range of frequencies over which the channel can be considered flat [4].

Results show values of RMS delay spread that are in the order of 100 ns and coherence bandwidth (at 50% correlation) in the range of 1 MHz as shown in Table III.

Channel Capacity

Channel capacity is a measure of the theoretical maximum data rate per unit of bandwidth that can be reliably transmitted through a certain channel [5]. SISO channel capacity is derived from measurements using equation (5) [3].

$$C_N[bps/Hz] = log_2(1 + \rho|H|^2). \qquad (5)$$

H is the normalized channel response and ρ is the average signal to noise ratio (SNR).

The results show that the channel capacity for a channel with a strong line of sight (LOS) component (belt-chest channel) is higher than the other channels with less strong LOS component. This result is consistent both for the average channel capacity (in Table.1) and for the CDF plots at a certain probability level (Fig.2). This is expected since a strong LOS component would result in a higher received power magnitude, and hence a higher SNR value. Detailed results for the average channel capacity are listed in Table 1.

Table 1. Parameters values for each channel

Parameters	Measurement Channels		
	Belt-chest	Belt-head	Belt-wrist
Average channel Capacity (bps/Hz)	9.0779	5.4376	3.7368
Coherence bandwidth at 50% correlation (MHz)	1.7	1.1	0.808
Coherence bandwidth at 90% correlation (MHz)	0.17	0.11	0.0808
RMS delay spread (ns)	117.1862	187.9793	247.6367

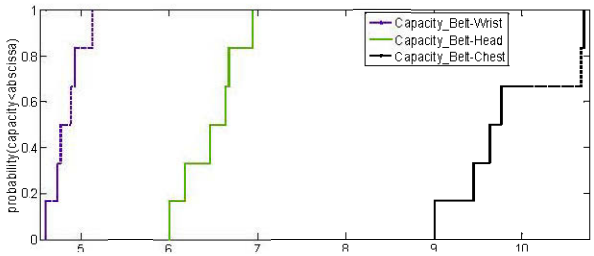

Figure 2. Capacity CDFs for the three on-body channels.

CONCLUSION

Three SISO on-body channel in a mine gallery has been characterized. The belt -chest channel is characterized by a strong LOS component. Hence, its channel capacity is higher than that of the belt-head and the belt-wrist channels; this is explained by the higher received power, and hence the SNR, when a strong LOS component is present. The RMS delay spreads and coherence bandwidths are close for the belt-head and the belt-wrist on-body channels (but worse than those of the belt-chest), suggesting that these two channels could be considered flat for about the same range of frequencies.

REFERENCES

[1]. Khan, P. S. Hall, A. A. Serra, A. R. Guraliuc, and P. Nepa, "Diversity Performance Analysis for On-Body Communication Channels at 2.45 GHz," IEEE Trans. Antennas Propag., vol. 57, no. 4, pp. 956-963, Apr. 2009.

[2]. Huan-Bang Li; Hamaguchi, K., "A prototype BAN for medical and healthcare monitoring based on high band UWB," *Wireless Personal Multimedia Communications (WPMC), 2011 14th International Symposium on* , vol., no., pp.1,5, 3-7 Oct. 2011

[3]. Inanoglu, Hakan, "Multiple-Input Multiple-Output System Capacity: Antenna and Propagation Aspects," *Antennas and Propagation Magazine, IEEE* , vol.55, no.1, pp.253,273, Feb. 2013 doi: 10.1109/MAP.2013.6474541

[4]. Rappaport, T.S.: 'Wireless communications: principle and practice' (Prentice Hall, 2001, 2nd edn)

[5]. Lee, W. C Y, "Estimate of channel capacity in Rayleigh fading environment," *Vehicular Technology, IEEE Transactions on* , vol.39, no.3, pp.187,189, Ang 1990

Off-Body Channel Characterization at 2.45 GHz in a Mine Evironment

Moulay El Azhari[1], Mourad Nedil[1], Ismail Ben Mabrouk[2]
1:Underground Communications Research Laboratory
UQAT, Val d'Or, Canada
2: Sensor Networks and Cellular Systems (SNCS) Research Center
University of Tabuk, Tabuk, Saudi Arabia

Abstract: In this paper, the off-body performance of a single-input single-output (SISO) system in a mine gallery was evaluated. Measurement campaigns using Monopole antennas have been taken in a gold mine for a line of sight topology. The off-body channel was characterized in terms of the channel impulse response, path loss, RMS delay spread, coherence bandwidth, and channel capacity.

Keywords: SISO, on-body channel, channel capacity, frequency response,impulse response.

I. INTRODUCTION

WBAN refers to the wireless communication technology which deals with the propagation at the on-body, off-body, and in-body channel. This growing technology has found many applications in the biomedical therapy, health care, and entertainment (mainly to transfer body information data) [1].

Many researchers have been performed to investigate the performance of the off-body channel at the 2.45 GHz ISM band, in the past few years, benefitting from the technological advancements that allow the use of this technology in small portable electronic devices [2].

The 2.45 GHz band has been thoroughly investigated for applications in a mine gallery, for regular radio transmission (not involving the human body), using different kinds of antennas such as the monopole and the patch antennas [3].

In this paper, the off-body channel is studied at the 2.45 GHz band using monopole antennas for LOS situations. The impulse responses were determined for different access points to body distances. The path loss was determined and sketched for different distances. The path loss exponent was then derived. Moreover, the channel capacity was calculated from measurements using the Shannon equation in [4]. The coherence bandwidth and RMS delay spread were also derived. The proposed measurement procedure is briefly discussed in section II and the results are provided in section III.

II. MEASUREMENT PROCEDURE

In order to characterize the off-body SISO channel in a mine gallery at 2.45 GHz, a transmitting antenna was placed at a fixed position in the middle of the mine gallery pathway (40m underground). The receiving antenna is placed on the right side of the chest of a 1.80m, 70Kg student wearing a miner's outfit. 6 data snap shots are taken at each distance, starting from a distance of 1m to a final position of 5m away from transmitter, as shown in Fig.1. The transmitting and receiving antennas were connected to the two ports of the previously calibrated vector network analyzer (VNA). At each snapshot, the S_{21} values are recorded for 6401 frequency samples. The noise floor for the measurements was considered at -90dBm. The environment mainly consists of very rough and dusty walls, floor, and ceiling. The temperature is about 6° C in a highly humid environment. There is mining machinery few meters away from the measurement' setup; the ceiling includes many metal rods and is covered with metal screens.

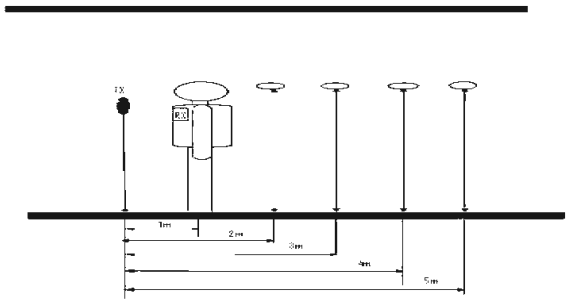

[1] Measurement setup

III. RESULTS

A. Channel impulse response

An inverse Fourier was applied to the average of six measured S_{21} sets of values (at each distance) in order to get impulse responses. As expected, the line of sight signal carries the highest power among the multipath received signals. In addition, the LOS component is stronger for the smaller transmitter-receiver (Tx-Rx) separations, and gradually lessens in value as we increase this separation.

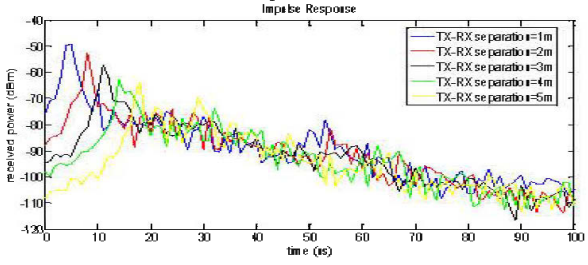

Figure 2. Impulse responses for the different Tx-Rx separations.

B. Path loss

The path loss was obtained from the path gains, by averaging over the frequencies samples and the different snapshots as shown in equation (1) [1].

$$PL(d(p)) = -20log_{10}\frac{1}{N_s N_f}\sum_{j=1}^{N_s}\sum_{n=1}^{N_f}\left|H_j^p(n)\right| \qquad (1)$$

Where $PL(d(p))$ is the path loss at the at the position of p (with TX-Rx separation $d(p)$); Ns and Nf are the number of the snapshots and frequency samples, respectively. $H_j^p(n)$ denotes the measured $S21$ for the position p, jth snapshot, and nth frequency sample[1].

The path loss is modeled as a function of the Tx-Rx distance [3] as shown in equation (2).

$$PL(d) = PL_{dB}(d_0) + 10.\alpha.log_{10}\left(\frac{d}{d_0}\right) + X \qquad (2)$$

Where $PL_{dB}(d_0)$ is the mean path loss at the reference distance d_0 , d is the distance where the path loss is calculated, α is the path loss exponent (determined using least square linear regression analysis), and X is a zero mean Gaussian variable (in dB) [3].

The path loss results and a linear regression of these values are plotted in fig.2.

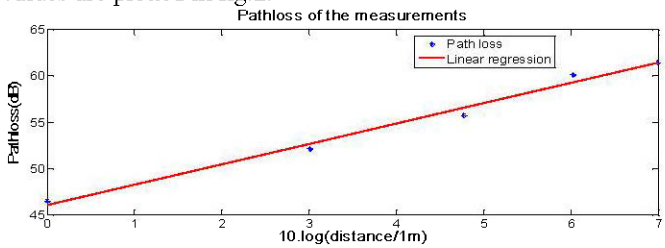

Figure 3. Path Loss values and their linear regression

From the above linear regression analysis, the path loss exponent α was found to be 2.1894. This value is a little bit over the path loss exponent at free space (which is equal to 2), due to multipath effects.

C. RMS delay spread and Coherence bandwidth

The the RMS delay spread (a parametter that quantifies the time dispersive properties of a multipath channel) was determined using equations in [5]. The Coherence bandwidth (a statistical measure of the range of frequencies over which the channel can be considered flat) was also calculated for 50% correlation using the equation in [5].

Results show values of RMS delay spread that are between 15ns and 66 ns and coherence bandwidth (at 50% correlation) in the range of 3-14 MHz as shown in Fig.3.

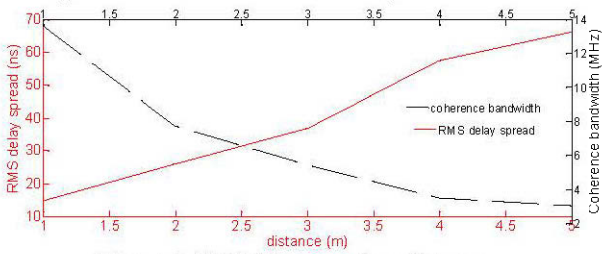

Figure 4: RMS delay spread vs. distance

D. Channel Capacity

SISO channel capacity (plotted in fig.4 and fig.5) is derived from measurements using Shannon formula (3) [3].

$$C_N[bps/Hz] = log_2(1 + \rho|H|^2). \qquad (3)$$

H is the normalized channel response and ρ is the average signal to noise ratio (SNR).

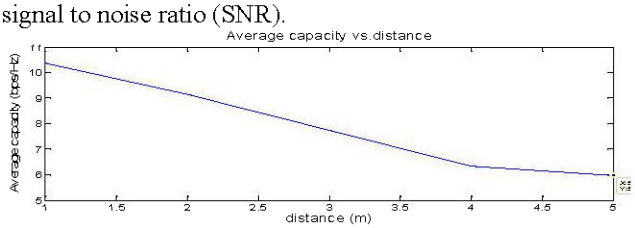

Figure 5. Average capacity vs. distance

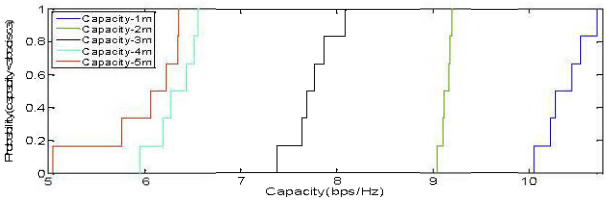

Figure 6. Capacity CDFs for the five off-body channel 'distances

As expected, the average capacity and the capacity at a certain probability level decreases with distance. This is explained by the fact that the smaller distances correspond to a higher received power and hence a higher SNR.

IV. CONCLUSION

A SISO off-body channel in a mine gallery has been characterized. From the results, a path loss exponent of 2.1894 was obtained (close to that of free space). The capacity for lower Tx-Rx separations is stronger than that of higher separations, due to the stronger received signal at small distances from the transmitter. The RMS delay spreads increases when Tx-Rx separation increases, while the coherence bandwidth decreases with distance.

REFERENCES

[1]. A.-M. Gao, Q. H. Xu, H.-L. Peng, W. Jiang, and Y. Jiang, "PERFORMANCE EVALUATION OF UWB ON-BODY COMMUNICATION UNDER WIMAX OFF-BODY EMI EXISTENCE," *Progress In Electromagnetics Research*, Vol. 132, 479-498, 2012.

[2]. Kvist, S.H.; Medina, P.F.; Thaysen, J.; Jakobsen, K.B., "On-body and off-body 2.45 GHz MIMO communications for hearing instrument applications," *Antennas and Propagation (EuCAP), 2013 7th European Conference on* , vol., no., pp.2595,2599, 8-12 April 2013

[3]. Ben Mabrouk, I.; Talbi, L.; Nedil, M.; Hettak, K. "MIMO-UWB Channel Characterization Within an Underground Mine Gallery", *Antennas and Propagation, IEEE Transactions on,* On page(s): 4866 - 4874 Volume: 60, Issue: 10, Oct. 2012

[4]. Inanoglu, Hakan, "Multiple-Input Multiple-Ontput System Capacity: Antenna and Propagation Aspects," *Antennas and Propagation Magazine, IEEE* , vol.55, no.1, pp.253,273, Feb. 2013

[5]. Rappaport, T.S.: 'Wireless communications: principle and practice'(Prentice Hall, 2001, 2nd edn)

ANNEXE B: Articles in the Process of Publishing

- M. ELazhariri, M. Nedil, I.Benmabrouk, K. Ghanem, and L. Talbi " Characterization of an Off-Body MIMO Channel at 2.45 GHz in a Mine Evironment" , *Antennas and Propagation, IEEE Transactions*, work In progress

- M. ELazhariri, M. Nedil, I.Benmabrouk, K. Ghanem, and L. Talbi " On-Body MIMO Channel Characterization at 2.45 GHz in a Mine Evironment" , *Antennas and Propagation, IEEE Transactions*, work In progress